ANALYTICAL STUDY OF CATALYTIC REACTORS FOR HYDRAZINE DECOMPOSITION: ONE-AND TWO-DIMENSIONAL STEADY-STATE PROGRAMS

E.J. SMITH, D.B. SMITH and A.S. KESTEN

AUGUST, 1968

Prepared for
NATIONAL AERONAUTICS AND SPACE ADMINISTRATION
CONTRACT NAS 7-458

United Aircraft Research Laboratories
UNITED AIRCRAFT CORPORATION

Abstract

Two machine computational programs have been developed under NASA Contract 7-458 to calculate the steady-state temperature and reactant concentration distributions in typical catalyzed hydrazine decomposition reaction chambers. One program is based upon a one-dimensional model of the reactor system which describes the behavior of reactors having radially uniform injection profiles and catalyst bed configurations, while the other program is based upon a two-dimensional model which permits consideration of nonuniform radial injection and of catalyst bed configurations exhibiting both radial and axial nonuniformities. The one and two-dimensional models and the computer programs developed from these models are described in detail in this computer manual. The manual contains operating instructions for these programs as well as descriptions of input and output formats. Also included is a discussion of possible operations problems which might arise together with appropriate means for solving these problems.

Foreword

This work was performed by United Aircraft Research Laboratories for the National Aeronautics and Space Administration under Contract NAS 7-458 initiated April 15, 1966.

Included among those who cooperated in performance of the work under NAS 7-458 were Dr. A. S. Kesten, Program Manager, Dr. W. G. Burwell, Chief, Kinetics and Thermal Sciences Section, Mr. D. B. Smith, Project Analyst, and Mrs. E. J. Smith, Applied Mathematician. This work was conducted under program management of the NASA Chief, Liquid Propulsion Experimental Engineering Systems, NASA Headquarters, Washington, D. C., and the Technical Manager was Mr. T. W. Price, Jet Propulsion Laboratory, Pasadena, California.

Summary

A description is contained herein of two machine computational programs developed under Contract NAS 7-458 with the National Aeronautics and Space Administration. These programs represent one- and two-dimensional steady-state models of catalyzed hydrazine decomposition reaction chambers. Both of these models consider both thermal and catalytic decomposition of reactants, along with simultaneous heat and mass transfer between the free-gas phase and the gas within the pores of the catalyst pellets. The one-dimensional model of the reactor system describes the behavior of reactors having radially uniform injection profiles and catalyst bed configurations, while the two-dimensional model permits consideration of nonuniform radial injection and of catalyst bed configurations exhibiting both radial and axial nonuniformities.

A general description of the one and two-dimensional models and a discussion of the machine programs developed from these models are contained in this manual. A description of input and output for both the one and two-dimensional steady-state programs are included in the discussion together with examples of typical data cases. Also included is a description of several operational problems which might be encountered while using the programs along with appropriate means for solving these problems. In addition, a short write-up of the subroutines contained in each deck is included along with general flow charts of the major routines.

1 Introduction

Under Contract NAS 7-458, the Research Laboratories of United Aircraft Corporation are performing analytical studies of the behavior of distributed-feed catalytic reactors for hydrazine decomposition. The specific objectives of this program are (a) to develop computer programs for predicting the temperature and concentration distributions in monopropellant hydrazine catalytic reactors in which hydrazine can be injected at arbitrary locations in the reaction chamber and (b) to perform calculations using these computer programs to demonstrate the effects of various system parameters on the performance of the reactor.

Progress previously reported in the first annual report (Ref. 1) included the development of a computer program which describes the steady-state behavior of a continuous flow type reactor system in which complete radial mixing in the free-gas (or liquid) phase was assumed. Progress previously reported in the second annual report (Ref. 2) included an extension of the steady-state program to include radial as well as axial

variations in temperature and concentrations in order to permit an analysis of various injection schemes and catalyst bed configurations which exhibit radial nonuniformities. These programs had been used to calculate temperature and reactant concentration distributions as functions of feed temperature, chamber pressure, mass flow rate distribution, catalyst size distribution, and embedded injector locations. As part of the third year of contract effort attention has been directed toward preparing a manual describing to potential users the operation of these computer programs. The manual includes a general description of the one and two-dimensional models as well as a detailed discussion of the machine programs representing these models.

2 Description of Analyses

The analysis of a hydrazine engine reaction system carried out to date pertains to a reaction chamber of arbitrary cross section packed with catalyst particles into which liquid hydrazine is injected at arbitrarily selected locations. Catalyst particles are represented as "equivalent" spheres with a diameter taken as a function of the particle size and shape. Both thermal and catalytic vapor phase decomposition of hydrazine and ammonia are considered in developing equations describing the concentration distributions of these reactants. Diffusion of reactants from the free-gas phase to the outside surface of the catalyst pellets is taken into account. Since the catalyst material is impregnated on the interior and exterior surfaces of porous particles, the diffusion of reactants into the porous structure must also be considered. In addition, the conduction of heat within the porous particles must be taken into account since the decomposition reactions are accompanied by the evolution or absorption of heat.

2.1 One-Dimensional Steady-State Model

In developing the one-dimensional steady-state model, the temperature and reactant concentrations in the interstitial phase (i.e., the free-fluid phase as distinguished from the gas phase within the porous particles) are assumed to vary only with axial distance along the bed. In the entrance region of the reaction chamber, where the temperature is low enough to permit the existence of liquid hydrazine, vaporization of liquid is assumed to occur as a result of decomposition of vapor hydrazine within the pores of the catalyst particles. That is, catalytic reaction is assumed to be fast enough to keep liquid hydrazine from wetting the pores of the particles; the hydrazine concentration at the surface of the catalyst particles at any axial location in the entrance region is then computed from the vapor pressure of liquid hydrazine in the interstitial phase at the same axial location. Neglecting axial diffusion of heat or mass, the change in enthalpy of the interstitial phase in the region where liquid hydrazine is present (i.e., where $h_i \leq h_i^V$) is related to the concentration gradient at the surface of the porous catalyst particles by

$$G\frac{dh}{dz} + H^{N_2H_4} D_p A_p \left(\frac{dC_P^{N_2H_4}}{dx}\right)_s + F(h_i - h_F) = 0 \quad \text{for } h_i \leq h_i^V \tag{1}$$

The variation of mass flow rate, G, with axial distance is easily computed from the rate of feed of liquid hydrazine from the distributed injectors into the system. In the region where liquid hydrazine exists at temperatures below the vaporization temperature, the temperature may be obtained from

$$T_i = T_F + \frac{h_i - h_F}{C_F} \quad \text{for } h_i < h_i^L \tag{2}$$

In the two-phase region, where $T_i = T_{vap}$, the weight-fraction of vapor may be computed from

$$\text{WEIGHT FRACTION VAPOR} = \frac{h_i - h_i^L}{h_i^V - h_i^L} \quad \text{for } h_i^L \leq h_i \leq h_i^V$$

At the axial position at which the enthalpy of the interstitial phase is just equal to the enthalpy of vapor hydrazine at the boiling point ($h_i = h_i^V$), the fraction of hydrazine injected upstream of that point which

has been decomposed is easily calculated from an overall heat balance. The associated amounts of ammonia, nitrogen, and hydrogen formed from decomposition of hydrazine can then be calculated taking the decomposition reaction as

$$2N_2H_4 \rightarrow 2NH_3 + N_2 + H_2 \tag{3}$$

It should be noted that this is the overall reaction scheme determined experimentally for both homogeneous decomposition of hydrazine (Refs. 3, 4, 5) and low pressure heterogeneous decomposition of hydrazine on platinum surfaces (Ref. 6).[1]

In the remainder of the reaction camber, where $h_i > h_i^V$, heat is being supplied to the system by homogeneous as well as heterogeneous decomposition of hydrazine. In addition, at sufficiently high temperature, heat is removed from the system by the endothermic decomposition of ammonia. For $h_i > h_i^V$ then, the change in enthalpy with axial distance is related to the reactant concentrations in the interstitial phase and at the surface of the porous catalyst particles by

$$\frac{dh_i}{dz} = -\frac{1}{G}\left\{F(h_i - h_F) + A_p h_c[T_i - (T_p)_s] + H^{N_2H_4} r_{hom}^{N_2H_4}\delta\right\} \tag{4}$$

The changes in reactant weight fractions in the interstitial phase with axial distance are related to the reactant concentrations in the interstitial phase and at the surface of the porous catalyst particles by

$$\frac{dw_i{}^{N_2H_4}}{dz} = \frac{1}{G}\left\{F - r_{hom}^{N_2H_4}\delta - A_p(k_c c_i)^{N_2H_4} - F\left(\frac{c_i}{\rho_i}\right)^{N_2H_4}\right\} \tag{5}$$

$$\begin{aligned}\frac{dw_i{}^{NH_3}}{dz} = \frac{1}{G}\Bigg\{ & r_{hom}^{N_2H_4}\delta\frac{M^{NH_3}}{M^{N_2H_4}} + A_p(k_c c_i)^{N_2H_4}\frac{M^{NH_3}}{M^{N_2H_4}} \\ & -A_P\left(k_c[c_i - (c_p)_s]\right)^{NH_3} - F\left(\frac{c_i}{\rho_i}\right)^{NH_3}\Bigg\}\end{aligned} \tag{6}$$

$$\begin{aligned}\frac{dw_i{}^{N_2}}{dz} = \frac{1}{G}\Bigg\{ & \frac{1}{2}r_{hom}^{N_2H_4}\delta\frac{M^{N_2}}{M^{N_2H_4}} + \frac{A_p}{2}(k_c c_i)^{N_2H_4}\frac{M^{N_2}}{M^{N_2H_4}} \\ & +\frac{A_p}{2}\left(k_c[C_i - (C_p)_s]\right)^{NH_3}\frac{M^{N_2}}{M^{NH_3}} - F\left(\frac{C_i}{\rho_i}\right)^{N_2}\Bigg\}\end{aligned} \tag{7}$$

$$\begin{aligned}\frac{dw_i{}^{H_2}}{dz} = \frac{1}{G}\Bigg\{ & \frac{1}{2}r_{hom}^{N_2H_4}\delta\frac{M^{H_2}}{M^{N_2H_4}} + \frac{A_p}{2}(k_c c_i)^{N_2H_4}\frac{M^{H_2}}{M^{N_2H_4}} \\ & +\frac{3A_p}{2}\left(k_c[c_i - (C_p)_s]\right)^{NH_3}\frac{M^{H_2}}{M^{NH_3}} - F\left(\frac{c_i}{\rho_i}\right)^{H_2}\Bigg\}\end{aligned} \tag{8}$$

where the film coefficients, h_c and k_c, may be estimated from (Ref. 7)

$$h_c = 0.74\left(\frac{G}{A_p\mu}\right)^{-0.41}(\overline{C}_F G) \tag{9}$$

$$k_c^j = \left(\frac{0.616}{\rho_i}\right)\left(\frac{\mu}{\rho_i D_i{}^J}\right)^{-0.667}\left(\frac{G}{A_p\mu}\right)^{-0.41} \tag{10}$$

[1]It is more commonly assumed, without benefit of experimental evidence, that the decomposition reaction is $3N_2H_4 \rightarrow 4NH_3 + N_2$, followed by dissociation of one of the four ammonia molecules to nitrogen and hydrogen. This two-step process leads to the same overall reaction cited above but assumes that a minimum of 25 percent of the ammonia produced by hydrazine decomposition also decomposes. The fractional ammonia dissociation, f, calculated assuming the validity of the two-step process is related by the fractional ammonia dissociation calculated in the present report by

$$(f)_{\text{two-step process}} = \frac{3}{4}(f)_{\text{present report}} + \frac{1}{4}$$

The changes in reactant concentrations with axial stance are then given by (THIS EQUATION NEEDS VERIFICATION WITH OTHER DOCUMENTS. IT'S NOT READABLE ON THE .PDF AND GEMINI DID THE BEST IT COULD.)

$$\frac{dc_i^j}{dz} = \rho_i \frac{dw_i^J}{dz} + w_i^j \frac{d\rho_i}{dz} \tag{11}$$

where

$$\frac{d\rho_i}{dz} = \rho_1 \left[\frac{1}{\overline{\overline{M}}} \frac{d\overline{M}}{dz} - \frac{1}{T_1} \frac{dT_1}{dz} + \frac{1}{P} \frac{dP}{dz} \right] \tag{12}$$

and

$$\frac{1}{\overline{\overline{M}}} \frac{d\overline{M}}{dz} = -\frac{1}{\sum_J \frac{w_1^J}{M^J}} \sum_J \frac{1}{M^J} \frac{dw_i^J}{dz} \tag{13}$$

$$\frac{dP}{dz} = -\left(\frac{1-\delta}{\delta^3} \right) \left(1.75 + \frac{150(1-\delta)}{2aG/\mu} \right) \left(\frac{G^2}{2a\rho_i g_c} \right) \tag{14}$$

The temperature of the interstitial phase in this region is related to the enthalpy by

$$h_i - h_i^V = \int_{T_{vap}}^{T_i} C_F dT_i \tag{15}$$

It should be noted that the hydrazine concentration at the surface of a catalyst particle in the vapor region, $(c_p)_s^{N2H4}$, is taken as zero. This reflects the fact that the catalytic reaction is so fast that the rate of decomposition is controlled by the rate of diffusion of hydrazine from the bulk vapor, through a stagnant gas film surrounding the catalyst particles, to the outside surface of the particles. In the case of ammonia, film diffusion is rapid relative to the rate of dissociation of ammonia within the particles. The concentration of ammonia at the surface of the catalyst particles, $(c_p)_s^{NH_3}$, is therefore fairly close to the ammonia concentrations in the bulk vapor phase, $c_i^{NH_3}$. The surface concentration can be calculated, along with the concentration profile in the porous particles, at any axial location by solving simultaneously the equations representing film and pore diffusion of heat and mass. In describing the diffusion of mass within a porous pellet, it is assumed that changes in the mass density of fluid within the particle are negligible relative to changes in concentration of the reacting species. In addition, pressure changes within the particle resulting from nonequimolar diffusion are neglected, as is heat transported by pore diffusion of mass. Assuming constant diffusion coefficients, D_p, and thermal conductivities, K_p, the equations describing heat and mass transfer within a catalyst particle may be written as

$$D_P^{NH_3} \nabla^2 c_p^{NH_3} - r_{het}^{NH_3} = 0 \tag{16}$$

$$K_p \nabla^2 T_p - H^{NH_3} r_{het}^{NH_3} = 0 \tag{17}$$

The boundary conditions which consider diffusion of heat, and mass through a film surrounding a spherical particle are

$$D_P^{NH_3} \left(\frac{dC_p}{dx} \right)_s^{NH_3} = k_c^{NH_3} \left[c_i^{NH_3} - (c_p)_s^{NH_3} \right] \tag{18}$$

and

$$(Hk_c c_i)^{N_2H_4} + H^{NH_3} D_p^{NH_3} \left(\frac{dc_p}{dx} \right)_s^{NH_3} = h_c [T_i - (T_p)_s] \tag{19}$$

Using Eqs. (16) and (17), Prater (Ref. 8) has pointed out that temperature and concentration are related quite simply by

$$T_p - (T_p)_s = \frac{HD_p}{K_p} [(c_p)_s - c_p] \tag{20}$$

The use of this relationship enables the reaction rate, r_{het}^{NH3}, to be written as a function of concentration alone instead of concentration and temperature. In this case, however, the reaction rate is a function of two parameters, $(T_p)_s$ and $(c_p)_s^{NH_3}$, which are yet to be determined. Equation 16 can be solved for the

concentration at any point in the porous particle in terms of the reaction rate, $r_{het}^{NH_3}$, and the interstitial concentration, $c_i^{NH_3}$. The solution is derived in Refs. 2 and 9 as an implicit integral equation given by

$$C_p(x) = c_i^{NH_3} - \left[\frac{1}{x} - \frac{ak_c^{NH_3} - D_p^{NH_3}}{a^2 k_c^{NH_3}}\right] \int_0^x \xi^2 \frac{r_{het}^{NH_3}(c_p)}{D_p^{NH_3}} d\xi \\ - \int_x^a \left[\frac{1}{\xi} - \frac{ak_c^{NH_3} - D_p^{NH_3}}{a^2 k_c^{NH_3}}\right] \xi^2 \frac{r_{het}^{NH_3}(c_p)}{D_p^{NH_3}} d\xi \tag{21}$$

In order to determine the particle ammonia concentration profile directly in terms of the interstitial temperature adn reactant concentrations it is necessary to solve Eqs. 18, 19 and 21 simultaneously. In the special case of negligible film resistance to heat and mass transfer (i.e. $(T_p)_s = T_i$ and $(c_p)_s = c_i$), Eq. (21) can be written, for any reacting species, as

$$C_p(x) = c_i - \left[\frac{1}{x} - \frac{1}{a}\right] \int_0^x \xi^2 \frac{r_{het}(c_p)}{D_p} d\xi - \int_x^a \left[\frac{1}{\xi} - \frac{1}{a}\right] \xi^2 \frac{r_{het}(c_p)}{D_p} d\xi \tag{22}$$

It is Eq. (22) which is used to describe the hydrazine concentration profiles within the catalyst particles located in the liquid region of the reaction chamber. In this liquid region it is assumed that liquid hydrazine wets the outside surface of the catalyst particles so that $(c_p)_s^{N2H4} = c_i^{N2H4}$, where c_i^{N2H4} is the vapor concentration in equilibrium with liquid hydrazine at temperature T_i. In the liquid-vapor region the situation is somewhat more complicated since it is difficult to predict whether liquid or a combination of liquid and vapor wets the outside surface of the catalyst particles. Both of these options are presently in the computer program representing the steady-state model. In the case in which both the liquid and vapor are taken to wet the particle surface, it is assumed that, at a given axial location, the fraction of the surface covered by vapor is equal to the weight-fraction of vapor present. Decomposition rates, computed assuming pure liquid surface coverage and then pure vapor coverage, are weighted accordingly. Fortuitously, for the system considered here, the liquid vapor region is so narrow that the choice of either of these options has negligible effect on the resulting temperature distributions (Ref. 1).

Finite difference methods have been used to program for digital computation the ordinary differential equations describing the changes in enthalpy and reactant concentrations in the interstitial phase. No iteration is necessary to solve these equations numerically when the incremental axial distances are sufficiently small. The size of a succeeding increment is calculated at each axial position as a function of the rates of change of temperature and fractional ammonia dissociation with axial distance. However, Eqs. (21) and (22), which must be solved simultaneously with the differential equations, are implicit integral equations which require iterative procedures for solution. Hand calculations have indicated that convergence to solutions for $c_p(x)$ are difficult to achieve unless the initial estimates of the concentration distributions are fairly accurate. Methods have been developed for generating these estimates and iterative procedures have been devised which effect rapid convergence over a fairly wide range of conditions. These procedures are presently used as subroutines in the main program representing the steady-state model.

2.2 Two-Dimensional Steady-State Model

In developing the two-dimensional steady-state model of a hydrazine reactor system the temperature and reactant concentrations in the bulk fluid phase are permitted to vary with radial and axial position in the reaction chamber. In the entrance region of the reactor, where the temperature is low enough to permit the existence of liquid hydrazine, radial mixing between adjacent layers of liquid is neglected. The equations representing the change in liquid enthalpy and temperature with axial distance at any radial position are the same as those developed for the one-dimensional model described previously. As in the one-dimensional model, catalytic reaction is assumed to be fast enough to keep liquid hydrazine from wetting the pores of the particles; the hydrazine concentration at the surface of the catalyst particles at any location in the entrance region is then computed from the vapor pressure of liquid hydrazine in the interstitial phase at the same location. In the vapor regions of the reaction chamber, turbulent diffusion of heat and mass is considered as a mechanism for radial mixing. Radial heat and mass fluxes are computed as functions of temperature and reactant concentration gradients. Heat is being supplied to the system by homogeneous as

well as heterogeneous decomposition of hydrazine, and is being removed from the system by the catalytic decomposition of ammonia.The change in enthalpy with axial distance at any radial location is related to the reactant concentrations in the interstitial phase and at the surface of the porous catalyst particles by

$$\frac{\partial h_i}{\partial z} = -\frac{1}{G}\left\{F(h_i - h_F) + A_p h_p[T_i - (T_p)_s] + H^{N_2H_4} r_{hom}^{N_2H_4}\delta + \frac{\partial q_r}{\partial r}\delta + \frac{q_r}{r}\delta + \frac{\partial T_i}{\partial r}\delta \sum_j N_r^j C_F^J\right\}^3 \tag{23}$$

The changes in reactant weight fractions in the interstitial phase with axial distance at any radial location are related to the reactant concentrations in the interstitial phase and at the surface of the porous catalyst particles by

$$\frac{\partial {w_i}^{N_2H_4}}{\partial z} = \frac{1}{G}\left\{F - r_{hom}^{N_2H_4}\delta - A_p(k_c c_i)^{N_2H_4} - \frac{\partial {N_r}^{N_2H_4}}{\partial r}\delta - \frac{N_r^{N_2H_4}}{r}\delta - F\left(\frac{c_i}{\rho_i}\right)^{N_2H_4}\right\} \tag{24}$$

$$\frac{\partial {w_i}^{NH_3}}{\partial z} = \frac{1}{G}\left\{r_{hom}^{N_2H_4}\delta\frac{M^{NH_3}}{M^{N_2H_4}} + A_p(k_c c_i)^{N_2H_4}\frac{M^{NH_3}}{M^{N_2H_4}} - A_p\left(k_c[c_i - (c_p)_S]\right)^{NH_3} - \frac{\partial N_r^{NH_3}}{\partial r}\delta - \frac{N_r^{NH_3}}{r}\delta - F\left(\frac{c_i}{\rho_i}\right)^{NH_3}\right\} \tag{25}$$

$$\frac{\partial {w_i}^{N_2}}{\partial z} = \frac{1}{G}\left\{\frac{1}{2}r_{hom}^{N_2H_4}\delta\frac{M^{N_2}}{M^{N_2H_4}} + \frac{A_P}{2}(k_c c_i)^{N_2H_4}\frac{M^{N_2}}{M^{N_2H_4}} + \frac{A_p}{2}\left(k_c[c_i - (c_p)_s]\right)^{NH_3}\frac{M^{N_2}}{M^{NH_3}} - \frac{\partial {N_r}^{N_2}}{\partial r}\delta - \frac{N_r^{N_2}}{r}\delta - F\left(\frac{c_i}{\rho_i}\right)^{N_2}\right\} \tag{26}$$

$$\frac{\partial {w_i}^{H_2}}{\partial z} = \frac{1}{G}\left\{\frac{1}{2}r_{hom}^{N_2H_4}\delta\frac{M^{H_2}}{M^{N_2H_4}} + \frac{A_p}{2}(k_c c_i)^{N_2H_4}\frac{M^{H_2}}{M^{N_2H_4}} + \frac{3A_p}{2}\left(k_c[c_i - (c_p)_s]\right)^{NH_3}\frac{M^{H_2}}{M^{NH_3}} - \frac{\partial N_r^{H_2}}{\partial r}\delta - \frac{N_r^{H_2}}{r}\delta - F\left(\frac{c_i}{\rho_i}\right)^{H_2}\right\} \tag{27}$$

where

$$q_r = -\lambda(\partial T_i/\partial r) \tag{28}$$

$$N_r^J = -\epsilon(\partial c_i^J/\partial r)_r \tag{29}$$

$$h_c = 0.74\left[\frac{G}{A_p\mu}\right]^{-0.41}[\overline{C}_F G] \tag{30}$$

$$k_c^J = \left[\frac{0.616}{\rho i}\right]\left[\frac{\mu}{\rho_i D_i^J}\right]^{-0.667}\left[\frac{G}{A_p\mu}\right]^{-0.41} \tag{31}$$

The eddy conductivity and diffusivity may be estimated from (Ref. 11)

$$\lambda = \frac{a\overline{C}_F G}{5\delta} \quad \text{and} \quad \epsilon = \frac{aG}{5\rho_i} \tag{32}$$

The changes in reactant concentrations with axial distance are then given by

$$\frac{\partial {c_i}^J}{\partial z} = \rho_i\frac{\partial {w_i}^J}{\partial z} + \frac{c_i^J}{\rho_i}\frac{\partial \rho_i}{\partial z} \tag{33}$$

[3]Equations of this type are presented in somewhat different form in Ref. 7. The last term on the right-hand side of the equation reflects the heat transferred by the radial diffusion of mass.

where

$$\frac{\partial \rho_i}{\partial z} = \rho_i \left[\frac{1}{\overline{M}} \frac{\partial \overline{M}}{\partial z} - \frac{1}{T_i} \frac{\partial T_i}{\partial z} + \frac{1}{P} \frac{dP}{dz} \right] \tag{34}$$

$$\frac{1}{\overline{M}} \frac{\partial \overline{M}}{\partial z} = - \frac{1}{\sum_J (w_i^J / M^J)} \sum_J \frac{1}{M^J} \frac{\partial {w_i}^J}{\partial z} \tag{35}$$

and the pressure drop may be estimated from the Ergun equation (Ref. 7) as

$$\frac{dp}{dz} = - \left(\frac{1-\delta}{\delta^3} \right) \left(1.75 + \frac{150(1-\delta)}{2aG/\mu} \right) \left(\frac{G^2}{2a\rho_i g_c} \right) \tag{36}$$

The mass flow rate, G, is computed as a function of the rate of feed of liquid hydrazine from the distributed injectors into the system. Bulk radial flow, caused by particle-fluid viscous interactions, is neglected. It is assumed, therefore, that downstream of the injectors the mass flow rate profile remains unchanged.

3 Discussion of One- and Two-Dimensional Steady-State Computer Programs

The equations representing the one and two-dimensional steady-state models have been programmed for the UNIVAC 1108 digital computer. These computer programs are discussed below. Included in this discussion are input and output descriptions and descriptions of common operational problems associated with the programs.

3.1 One-Dimensional Steady-State Model

3.1.1 Input Description

The following is a listing of the necessary input for the one-dimensional steady-state computer program. The input format is given in Table I. The coding of a sample data case is shown in Fig. 1 and a listing of the input data punch cards corresponding to this sample data case is shown in Fig. 2. The card numbers in the text below correspond to the card numbers (first column) of Table I. For each run there will be only one card number one. Cards 2 through 16 should be repeated for each data case to be run.

1. The first card contains the number **NCASE**. This number indicates the number of data cases with each run. $1 \leq$ NCASE ≤ 999.

2. The second card is the **title card** used for individual data case identification. The title may be any alpha numeric information desired.

3. The third card contains the indicators **OPTION** and **PRINT** and the number **NOFZ**. **OPTION** is used to indicate which method of analyzing the liquid-vapor region is desired. If **OPTION** = 2, the program will use the method in subroutine LQV2. If **OPTION** $\neq$ 2, the program will use the method in subroutine LQVP. These two methods are described in Appendix I. **PRINT** is used to indicate which type of printout is desired. If **PRINT** = 0 or is blank, the "standard output" described in the section on output is printed. If **PRINT** = 1, both "standard" and "nonstandard output" are printed. "Nonstandard output" is also described in the section on output. **NOFZ** is the number of axial stations (Z's) to be used in the three tables input on cards 8 through 16.

4. The fourth card contains the eight constants **ZO**, **GO**, **FC**, **ALPHA3**, **HF**, **R**, **WM4**, and **WM3**.

   - **ZO** is the axial distance to the end of a buried injector in ft. (Ref. 1).
   - **GO** is the inlet mass flow rate in $lb/ft^2 - sec$. It must be greater than zero.
   - **FC** is the rate of feed of hydrazine from buried injectors (Ref. 1) into the system in lb/ft^3-sec.
   - **ALPHA3** is the preexponential factor in the rate equation for the thermal decomposition of hydrazine (See Ref. 1). It equals $2.14 \times 10^{10} sec^{-1}$.

- **HF** is the enthalpy of liquid hydrazine entering the bed in Btu/lb.
- **R** is a gas constant. It equals 10.73 $(psia - ft^3)/(lb$ mole-deg $R)$.
- **WM4** is the molecular weight of hydrazine. It equals 32.048 lb/lb mole.
- **WM3** is the molecular weight of ammonia. It equals 17.032 lb/lb mole.

5. The fifth card contains the eight constants **WM2**, **WM1**, **ALPHAL**, **ALPHA2**, **AGM**, **BGM**, **KP**, and **CGM**.

   - **WM2** is the molecular weight of nitrogen. It equals 28.016 lb/lb mole.
   - **WM1** is the molecular weight of hydrogen. It equals 2.016 lb/lb mole.
   - **ALPHAL** is the preexponential factor in the rate equation for the catalytic decomposition of hydrazine (See Ref. 1). For the Shell 405 catalyst it equals $10^{10} sec^{-1}$.
   - **ALPHA2** is the preexponential factor in the rate equation for the catalytic decomposition of ammonia (See Ref. 1). For the Shell 405 catalyst it equals $10^{11}(lb/ft^3)^{0.5}(sec)^{-1}$. (Note: the exponent 1.b in the original file was 0.5 in the PDF)
   - **AGM** is the activation energy for the catalytic decomposition of hydrazine, divided by the gas constant. For the Shell 405 catalyst it equals 2500 deg R.
   - **BGM** is the activation energy for the catalytic decomposition of ammonia, divided by the gas constant. For the Shell 405 catalyst it equals 50,000 deg R.
   - **KP** is the thermal conductivity of the porous catalyst particle. For the Shell 405 catalyst it equals 0.4×10^{-4} Btu/ft-sec-deg R.
   - **CGM** is the activation energy for the thermal decomposition of hydrazine, divided by the gas constant. It equals 33,000 deg R.

6. The sixth card contains the seven constants **TF**, **CFL**, **ENMX1**, **ENMX2**, **ENMX3**, **DIF3**, **DIF4**, and the inlet value of **PRES**.

   - **TF** is the temperature of liquid hydrazine entering the bed in deg R.
   - **CFL** is the specific heat of liquid hydrazine. It equals 0.7332 Btu/lb-deg R.
   - **ENMX1** is the constant used to determine the size of axial station increments in the liquid region. It equals 200. Increasing this number would result in a decrease in size of axial station increments (and an increase in computer run time).
   - **ENMX2** is the constant used to determine the size of axial station increments in the liquid-vapor region. It equals 40. Increasing this number would result in a decrease in size of axial station increments (and an increase in computer run time).
   - **ENMX3** is the constant used to determine the size of axial station increments in the vapor region. It equals 80. Increasing this number would result in a decrease in size of axial station increments (and an increase in computer run time).
   - **DIF3** is the diffusion coefficient of ammonia in the gas phase at STP. It equals $0.17x10^{-3} ft^2/sec$.
   - **DIF4** is the diffusion coefficient of hydrazine in the gas phase at STP. It equals $0.95x10^{-4} ft^2/sec$.
   - **PRES** is the inlet chamber pressure in psia.

7. The seventh card contains the four constants **ZEND**, **EN1**, **EN2**, and **EN3**.

   - **ZEND** is the catalytic bed length in ft.
   - **EN1** is the order of hydrazine catalytic decomposition reaction with respect to hydrazine. For the Shell 405 catalyst it equals 1.0.
   - **EN2** is the order of ammonia catalytic decomposition reaction with respect to ammonia. For the Shell 405 catalyst it equals 1.0.

- **EN3** is the order of ammonia catalytic decomposition reaction with respect to hydrogen. For the Shell 405 catalyst it equals -1.6.

8. **Cards 8 through 10** contain **ZTBLA(I)**, the interpolation table used to obtain the catalyst particle radius (A) at any point along the reactor bed. Subroutine UNBAR, an interpolation routine developed at the United Aircraft Research Laboratories, is used to obtain an appropriate particle radius, A, for a given axial station, $Z(I)$, along the bed. For this table there should be a total of (NOFZ) Z's and (NOFZ) A's. The table is set up as follows:

   - **CARD NO. 8**: This card contains the four table descriptors used by UNBAR. The first descriptor signifies the table number. For this program it equals 0.0. The second descriptor tells at what location in the array the table starts; the tables in this program are read in such that this number equals 1.0. The third descriptor is the number of independent variables in the table (in this case, the number of Z's). This number equals NOFZ. The fourth descriptor for a univariate table such as this one should equal 0.0.
   - **CARD(S) NO. 9**: These cards contain the monotonically increasing Z values. Enough cards should be used to contain NOFZ values of Z at the rate of ten per card. For example, if NOFZ = 12, 12 values of Z should be input using two cards with ten values on the first card and the 2 remaining values on the second card.
   - **CARD(S) NO. 10**: These cards contain the A's which correspond to the Z's listed on cards 9. Enough cards should be used to contain NOFZ values of A at the rate of ten per card.

9. **Cards 11 through 13** contain **ZTBLAP(I)**, the interpolation table used to obtain the total external catalyst particle surface area per unit volume of bed (AP). These AP values are obtained from UNBAR as functions of axial distance (Z) as in the ZTBLA table discussed above. For this table there should be a total of (NOFZ) Z's and (NOFZ) AP's. The table is set up as follows:

   - **CARD NO. 11**: This card is exactly the same as card 8.
   - **CARD(S) NO. 12**: These cards are exactly the same as cards 9.
   - **CARD(S) NO. 13**: These cards contain the AP values which correspond to the Z's listed on cards 12. Enough cards should be used to contain NOFZ values of AP at the rate of ten per card.

10. **Cards 14 through 16** contain **ZTBLD(T)**, the interpolation table used to obtain the interparticle void fraction (DELA). These DELA values are obtained from UNBAR as functions of axial distance (Z) as in the ZTBLA table discussed above. For this table there should be a total of (NOFZ) Z's and (NOFZ) DELA's. The table is set up as follows:

    - **CARD NO. 14**: This card is exactly the same as card 8.
    - **CARD(S) NO. 15**: These cards are exactly the same as cards 9.
    - **CARD(S) NO. 16**: These cards contain the DELA values which correspond to the Z's listed on cards 15. Enough cards should be used to contain NOFZ values of DELA at the rate of ten per card.

3.1.2 Input Format

3.1.3 Output Description

Output from the one-dimensional steady-state program is entirely in printout form. Standard output, which is printed out when input option `PRINT = 0`, includes all printing normally done during execution of any representative data case, three messages which pertain to calculations which do not follow the normal pattern in a typical run, and one error message which is followed by program termination. Non-standard output is printed in addition to the standard output when `PRINT = 1`. This non-standard output includes additional calculated values and comments which pertain to intermediate calculations.

The print statements associated with each routine in which output is generated are described below.

Table 1: One-Dimensional Steady-State Computer Program Input Format

CARD NUMBER	NUMBER OF CARDS	FORMAT FORTRAN	USED COLUMNS	SYMBOL OR DESCRIPTION	SYMBOL USED IN EQUATIONS	NOMENCLATURE
1.	1	I3*	1-3	NCASE		No. of cases
2.	1	14A6	1-80	Title		
3.	1	2I2, I3*	1-2	OPTION		Liq. Vap. Indicator
			3-4	PRINT		Print Indicator
			5-7	NOFZ		No. of Z's in Input Tables

...

(*Note: The OCR for this table is heavily corrupted. The data must be manually transcribed from the original document.*)

(NONE OF THIS DATA WAS VERIFIED. WE JUST COPIED/PASTED FOR NOW. COME BACK TO THIS AND CHECK THE DATA.)

Table 2: Figure 1: Coding of a Sample Data Case (Reconstructed from Fig. 2)

Card	1.....10.....20.....30.....40.....50.....60.....70.....80
1	1
2	**SAMPLE DATA CASE (1-DIM SS)** MIXED BED G0= 3.0 P = 100.
3	1 0 20
4	0. 3.0 0. .214 E+11 0. 10.73 32.048 17.032
5	28.016 2.016 1.E+11 1.E+11 2500. 50000. .40 E-4 33000.
6	530. .7332 200. 40. 80. .17 E-3 .95 E-4 100.
7	.25 1. 1. -1.6
8	.0 1. 20. 0.
9a	0. .0055 .0111 .0167 .0168 .0439 .0575 .0711 .0847 .0983
9b	.1119 .1255 .1391 .1527 .1663 .1799 .1935 .2207 .2343 .2500
10a	.001 .001 .001 .001 .0064 .0064 .0064 .0064 .0064 .0064
10b	.0064 .0064 .0064 .0064 .0064 .0064 .0064 .0064 .0064 .0064
11	.0 1. 20. 0.
12a	0. .0055 .0111 .0167 .0168 .0439 .0575 .0711 .0847 .0983
12b	.1119 .1255 .1391 .1527 .1663 .1799 .1935 .2207 .2343 .2500
13a	2100. 2100. 2100. 2100. 330. 330. 330. 330. 330. 330.
13b	330. 330. 330. 330. 330. 330. 330. 330. 330. 330.
14	.0 1. 20. 0.
15a	0. .0055 .0111 .0167 .0168 .0439 .0575 .0711 .0847 .0983
15b	.1119 .1255 .1391 .1527 .1663 .1799 .1935 .2207 .2343 .2500
16a	.34 .34 .34 .34 .34 .34 .34 .34 .34 .34
16b	.34 .34 .34 .34 .34 .34 .34 .34 .34 .34

Table 3: Listing of Input Data Punch Cards: Sample Case (from Fig. 2)

Card Number	Data / Values
Card 1	1
Card 2	**SAMPLE DATA CASE (1-DIM SS)** MIXED BED G0= 3.0 P = 100.
Card 3	1 0 20
Card 4	0. 3.0 0. .214 E+11 0. 10.73 32.048 17.032
Card 5	28.016 2.016 1.E+11 1.E+11 2500. 50000. .40 E-4 33000.
Card 6	530. .7332 200. 40. 80. .17 E-3 .95 E-4 100.
Card 7	.25 1. 1. -1.6
Card 8	.0 1. 20. 0.
Card 9a	0. .0055 .0111 .0167 .0168 .0439 .0575 .0711 .0847 .0983
Card 9b	.1119 .1255 .1391 .1527 .1663 .1799 .1935 .2207 .2343 .2500
Card 10a	.001 .001 .001 .001 .0064 .0064 .0064 .0064 .0064 .0064
Card 10b	.0064 .0064 .0064 .0064 .0064 .0064 .0064 .0064 .0064 .0064
Card 11	.0 1. 20. 0.
Card 12a	0. .0055 .0111 .0167 .0168 .0439 .0575 .0711 .0847 .0983
Card 12b	.1119 .1255 .1391 .1527 .1663 .1799 .1935 .2207 .2343 .2500
Card 13a	2100. 2100. 2100. 2100. 330. 330. 330. 330. 330. 330.
Card 13b	330. 330. 330. 330. 330. 330. 330. 330. 330. 330.
Card 14	.0 1. 20. 0.
Card 15a	0. .0055 .0111 .0167 .0168 .0439 .0575 .0711 .0847 .0983
Card 15b	.1119 .1255 .1391 .1527 .1663 .1799 .1935 .2207 .2343 .2500
Card 16a	.34 .34 .34 .34 .34 .34 .34 .34 .34 .34
Card 16b	.34 .34 .34 .34 .34 .34 .34 .34 .34 .34

Standard Output

- **MAIN program**

  1. A complete listing of all program input including FORTRAN variable titles for all input variables.
  2. Axial position, (Z), temperature, (TEMP), enthalpy, (H), and rate of change of enthalpy with axial distance, (DHDZ), for each axial position in the liquid region.

- **Subroutine LQVP or LQV2**

  1. Axial position, (Z), temperature, (TEMP), enthalpy, (H), and weight fraction of vapor, (WFV), for each axial position in the liquid-vapor region.

- **Subroutine VAPOR**

  1. Axial position, (Z), temperature, (TEMP), pressure (PRES), enthalpy, (H), and concentrations of hydrogen, (C1), nitrogen, (C2), ammonia, (C3), and hydrazine, (C4), at each axial position in the vapor region.
  2. Mole fractions of hydrogen, (MFRAC1), nitrogen, (MFRAC2), ammonia, (MFRAC3), and hydrazine, (MFRAC4), and the fractional dissociation of ammonia, (FRAC3D), at each axial position in the vapor region.
  3. All axial positions, (Z values), in the vapor region listed consecutively and MBAR and G values at the end of the reactor for use in preparing input to the transient model computer program.
  4. "KOUNT = XX — THIS INTERVAL HAS BEEN REDIVIDED XXXX TIMES"
     For all cases involving a non-zero embedded injector feed rate, a check is made on the Z step size after each calculation. If the increment proves too large to yield satisfactory results, it is halved and re-checked. The procedure continues until a satisfactory interval size is found, and the above message is then printed.

5. "THERE IS A PUDDLE OF COLD HYDRAZINE AT THE LIQUID-VAPOR/VAPOR INTERFACE.— TRY USING A LARGER VALUE FOR GO"

   When using a buried injector scheme it is possible to "flood" the region surrounding the injector tip with cold, liquid hydrazine. A sudden drop in axial temperatures at the liquid-vapor/vapor interface indicates that this has occurred, and in such cases the above message is printed and no further calculations are made.

- **Subroutine SGRAD**

1. "WE HAVE CALCULATED A NEGATIVE XO DURING ITERATION NO. XX. SET $X0 = 0$, CALCULATE TPS = .XXXXX + XX, AND CONTINUE"

   X0 represents an approximation of the radial distance to which hydrazine penetrates the catalyst particle before being dissipated. It is determined through an iterative procedure, and in some instances initial guesses do not yield satisfactory results. In this case, corrective measures to yield a better approximation to XO are instituted and the procedure repeated. This message indicates only that corrective calculations to improve on the accuracy of XO are being initiated.

2. "UNABLE TO CONVERGE ON CPS IN 50 TRIES — $CP(X/A) = .xxxxxx \pm xx$"

   If subroutine SGRAD cannot calculate a "converged" value for CPS after 50 iterations, the final value for CP at the particle surface is used to approximate CPS. This is a good approximation to CPS, however, and program calculations continue with the above message being printed.

3. "UNABLE TO FIND SUITABLE X0 AFTER FOUR TRIES OF 25 ITERATIONS EACH — PROGRAM STOP FOLLOWS"

   If after four corrective attempts to approximate X0 the procedure still do not yield satisfactory results, this message along with all unacceptable values for X0 is printed and further calculations are stopped. An octal dump of core accompanies the program stop.

Non-Standard Output

- **Subroutine SLOPE**

1. "INITIAL CHOICE THROUGH ORIGIN IS TOO LARGE"

   When iterating to find a satisfactory approximation to the radial depth of penetration of hydrazine in a catalyst particle (X0 calculation), an initial guess is the particle radius itself. If this proves to be an unsatisfactory choice, the above message is printed and a different initial guess is used.

2. "SATISFACTORY STARTING CURVE FOUND AFTER XX TRAILS. THE VALUE OF B (X0) IS .XXXXXX + XX"

   This message indicates that a satisfactory approximation to the radial depth of penetration of hydrazine in a catalyst particle has been found, and appears frequently in calculations involving the liquid region of the reactor.

3. "INITIAL CHOICE THRU ORIGIN SEEMINGLY OK, BUT RESULTS ROTTEN AFTER 99 ITERATIONS — SET X0 =.000001* A AND USE MORE REFINED TECHNIQUE"

   When calculating a concentration vs radial position profile within the catalyst particle, an initial guess at the profile is used assuming a linear profile from the center of the particle to the surface. It can happen that this appears to be a satisfactory first guess, but ultimately yields unsatisfactory results for the final "converged" values of CPA. In such instances the above message is printed and the iteration procedure is repeated using a new initial guess.

4. "ITERATION = XX

X/A	CPA	X/A	CPA	X/A	CPA	X/A	CPA
XXXX	XXXX	XXXX	XXXX	XXXX	XXXX	XXXX	XXXX
XXXX	XXXX	XXXX	XXXX	XXXX	XXXX	XXXX	XXXX
:	:	:	:	:	:	:	:
XXXX	XXXX	XXXX	XXXX	XXXX	XXXX	XXXX	XXXX

   THE SLOPE CONVERGES TO XXXXXXX + xx"

When a converged value for the slope of the concentration profile curve at the catalyst particle surface has been calculated, the above "concentration profile" will be printed. The word "ITERATION" refers to the iteration count at the time of convergence. X/A is the normalized distance from the center of the catalyst particle of radius A to the surface. CPA is the concentration of hydrazine within the particle at the corresponding normalized radial distance. The final message indicates the final converged value of the slope. This block will be printed for each axial station of the liquid region.

5. "THE SLOPE CONVERGES TO $.xxxxxx \pm xx$"

   This message indicates that the iterative procedure has achieved convergence on a value of the hydrazine concentration gradient at the catalyst particle surface, and appears frequently in calculations involving the liquid region of the reactor.

- **Subroutine SGRAD**

1. A listing of converged reactant concentration ($CP(X/A)$) versus normalized radial distance within the catalyst particle (X/A) at each axial position in the vapor region.

2. (a) "CONCENTRATION GRADIENT FOUND AFTER XXX TRIES"
   (b) "$CP(X)$ AT PARTICLE SURFACE $.xxxxxx \pm xx$"
   (c) "KC3* (C13-CPS) = $.xxxxxx \pm xx$"
   (d) "HC* (T-TPS)= $.xxxxxx \pm xx$"

   Print message (a) indicates the number of iterations that were needed to find a converged value for the concentration gradient.

   Print message (b) gives the converged value for the concentration at the particle surface $(c_p)_s$.

   Print messages (c) and (d) give calculated values where KC3 is the mass transfer coefficient for ammonia, CI3 is the interstitial concentration of ammonia at the catalyst surface, HC is the heat transfer coefficient, T is the interstitial temperature, and TPS is the temperature at the surface of the catalyst.

   Print messages (a), (b), (c), and (d) appear at each axial position in the vapor region.

3. "SATISFACTORY XO FOUND AFTER XXX TRIES, X0 = $.xxxxxx \pm xx$"

   When calculating an ammonia concentration radial profile within a catalyst particle it is necessary to determine the radial depth of penetration of ammonia. The approximate radial position of "zero" concentration is referred to as XO in subroutine SGRAD, and when the iterative procedure employed has successfully determined a value of XO, the above message, with iteration count, is printed.

A sample listing of the output for a typical one-dimensional steady-state data case is shown in Figs. 3a through 3f.

Common Operational Problems

Many different data cases have been run with the one-dimensional steady-state computer program. During these runs, most of the problems which have developed have been eliminated through program modification. However, two problems which may still occur are noted below, together with appropriate techniques for solving them.

1. "UNABLE TO FIND SUITABLE X0 AFTER FOUR TRIES OF 25 ITERATIONS EACH — PROGRAM STOP FOLLOWS"

   If a satisfactory value for X0 cannot be found after four attempts, this message is printed and program execution is terminated. An appropriate solution to this problem would be to try different values for f_i [Eq. (I-11) in discussion of SGRAD, Appendix I]. These values could be greater than 0.95. To make this change, subroutine SGRAD would have to be recompiled using the new values of f_i.

2. "THERE IS A PUDDLE OF COLD HYDRAZINE AT THE LIQUID-VAPOR/VAPOR INTERFACE — TRY USING A LARGER VALUE FOR G0"

When using a buried injector scheme it is possible to "flood" the region surrounding the injector tip with cold, liquid hydrazine. A sudden drop in axial temperatures at the liquid-vapor/vapor interface indicates that this has occurred, and in such cases the above message in printed and no further calculations are made. An appropriate solution to this problem would be to try a larger input value for GO and rerun the program with the revised input.

Figures 3a-3f: Listing of Output for Sample Data Case

Table 4: Listing of Output for Sample Data Case (Figs. 3a-3f)

Sample Data Output

```
**SAMPLE DATA CASE (1-DIM SS)** MIXED BED G0= 3.0 P = 100.
000000
INPUT CONSTANTS
HL HV TF TVAP CFL PRESSURE KP F G0
.212628+03 .715478+03 .530000+03 .820000+03 .733200-00 .100000+03 .400000-04 .000000 .300000+01
R ALPHA3 CGM DIF3 DIF4 WM4 WM3 WM2 WM1 ZEND
.107300+02 .214000+11 .330000+05 .170000-03 .950000-04 .320480+02 .170320+02 .280160+02 .201600+01 .250000+00
AGM BGM ALPHA1 ALPHA2 N1 N2 N3 ENMX1 ENMX2 ENMX3
.250000+04 .500000+05 .100000+12 .100000+11 .100000+01 .100000+01 -.160000+01 .200000+03 .400000+02 .800000+02
000000
ZO
.000000
Z VS A TABLE
.000000 .100000+01 .200000+02 .000000
.000000 .550000-02 .111000-01 .167000-01 .168000-01 .439000-01 .575000-01 .711000-01 .847000-01 .983000-01
.111900+00 .125500+00 .139100+00 .152700+00 .166300+00 .179900+00 .193500+00 .207100+00 .220700+00 .234300+00
.100000-02 .100000-02 .100000-02 .100000-02 .640000-02 .640000-02 .640000-02 .640000-02 .640000-02 .640000-02
.640000-02 .640000-02 .640000-02 .640000-02 .640000-02 .640000-02 .640000-02 .640000-02 .640000-02 .640000-02
Z VS AP TABLE
.000000 .100000+01 .200000+02 .000000
.000000 .550000-02 .111000-01 .167000-01 .168000-01 .439000-01 .575000-01 .711000-01 .847000-01 .983000-01
.111900+00 .125500+00 .139100+00 .152700+00 .166300+00 .179900+00 .193500+00 .207100+00 .220700+00 .234300+00
.210000+04 .210000+04 .210000+04 .210000+04 .330000+03 .330000+03 .330000+03 .330000+03 .330000+03 .330000+03
.330000+03 .330000+03 .330000+03 .330000+03 .330000+03 .330000+03 .330000+03 .330000+03 .330000+03 .330000+03
Z VS DELTA TABLE
.000000 .100000+01 .200000+02 .000000
.000000 .550000-02 .111000-01 .167000-01 .168000-01 .439000-01 .575000-01 .711000-01 .847000-01 .983000-01
.111900+00 .125500+00 .139100+00 .152700+00 .166300+00 .179900+00 .193500+00 .207100+00 .220700+00 .234300+00
.340000-00 .340000-00 .340000-00 .340000-00 .340000-00 .340000-00 .340000-00 .340000-00 .340000-00 .340000-00
.340000-00 .340000-00 .340000-00 .340000-00 .340000-00 .340000-00 .340000-00 .340000-00 .340000-00 .340000-00

****************************** ENTERING LIQUID REGION ******************************

 Z TEMP H DHDZ
```

Continued on next page

Table 4 – continued from previous page

Sample Data Output

```
.00000000 .530000+03 .000000 .377541+05
.251216-03 .542936+03 .189619+02 .538926+05
.484469-03 .555662+03 .379026+02 .945157+05
.527298-03 .568781+03 .568781+02 .343787+06
.593145-03 .581695+03 .757274+02 .221126+06
.635941-03 .594602+03 .946115+02 .322530+06
.665267-03 .607502+03 .113477+03 .467775+06
.665477-03 .620396+03 .132323+03 .675305+06
.699470-03 .633283+03 .151168+03 .962125+06
.709286-03 .646164+03 .169992+03 .132107+07
.716432-03 .659039+03 .188824+03 .183241+07
.721580-03 .671907+03 .207641+03 .242181+07
.725474-03 .684769+03 .226450+03 .316562+07
.728452-03 .697625+03 .245250+03 .412827+07
.730734-03 .710474+03 .264042+03 .577362+07
.732365-03 .723316+03 .282827+03 .750974+07
.733618-03 .736154+03 .301605+03 .935122+07
.734627-03 .748989+03 .320377+03 .117621+08
.735427-03 .761822+03 .339146+03 .151422+08
.736046-03 .774653+03 .357912+03 .187859+08
.736547-03 .787482+03 .376676+03 .225211+08
.736964-03 .800310+03 .395438+03 .269846+08
.737323-03 .813133+03 .414199+03 .342904+08
.737459-03 .820000+03 .423306+03 .383323+08

************************** ENTERING LIQUID VAPOR REGION **************************

.73770-03 .82000+03 .25963+03 .093472-01
.73895-03 .82000+03 .30663+03 .18594-00
.74016-03 .82000+03 .35363+03 .28041-00
.74138-03 .82000+03 .40064+03 .37389-00
.74261-03 .82000+03 .44764+03 .46796-00
.74384-03 .82000+03 .49464+03 .56083-00
.74506-03 .82000+03 .54164+03 .65430-00
.74629-03 .82000+03 .58865+03 .74777-00
```

Continued on next page

Table 4 – continued from previous page

Sample Data Output

```
.74751-03 .82000+03 .63565+03 .84124-00
.74874-03 .82000+03 .68265+03 .93472-00
.75082-03 .82000+03 .71548+03 .10000+01

**************************** ENTERING VAPOR REGION ****************************

Z= .075082274-03 TEMP= .82000000+03 PRES= .10000000+03 H= .71547795+03
C1= .31579918-02 C2= .43586062-01 C3= .53360037-01 C4= .10343207-00
MFRAC1= .13782692-00 MFRAC2= .13782692-00 MFRAC3= .27565384-00 MFRAC4= .44869231-00 FRAC3D= -.00000000

Z= .090740574-03 TEMP= .86645369+03 PRES= .99981377+02 H= .73897909+03
C1= .32506140-02 C2= .43334669-01 C3= .50454650-01 C4= .15041867-00
MFRAC1= .14429730-00 MFRAC2= .14429730-00 MFRAC3= .27635187-00 MFRAC4= .42893217-00 FRAC3D= .21670607-01

Z= .10665796-02 TEMP= .91158767+03 PRES= .99960899+02 H= .76246590+03
C1= .33173617-02 C2= .42790974-01 C3= .48003883-01 C4= .13356108-00
MFRAC1= .16197901-00 MFRAC2= .15034878-00 MFRAC3= .27743711-00 MFRAC4= .41023511-00 FRAC3D= .40233626-01

Z= .12278735-02 TEMP= .95559712+03 PRES= .99938571+02 H= .78594348+03
C1= .33603019-02 C2= .42236826-01 C3= .45931103-01 C4= .12162228+00
MFRAC1= .17243814-00 MFRAC2= .15596628-00 MFRAC3= .27898882-00 MFRAC4= .39260677-00 FRAC3D= .55749761-01

...  (Data continues) ...

Z= .17155202-00 TEMP= .19507243+04 PRES= .78863929+02 H= .14092872+04
C1= .39661221-02 C2= .31522408-01 C3= .96198352-02 C4= .00000000
MFRAC1= .53774555-00 MFRAC2= .30754914-00 MFRAC3= .15470531-00 MFRAC4= .00000000 FRAC3D= .59806513-00

Z= .24999999-00 TEMP= .19053842+04 PRES= .71680713+02 H= .13780029+04
C1= .38096090-02 C2= .29667359-01 C3= .77733879-02 C4= .00000000
MFRAC1= .55496938-00 MFRAC2= .31099591-00 MFRAC3= .13403673-00 MFRAC4= .00000000 FRAC3D= .64541664-00

Z'S FROM VAPOR REGION
.7508227-03 .9074057-03 .1066580-02 .1227874-02 .1392110-02 .1559678-02 .1730142-02 .1905576-02 .2084807-02 .2269192-02
.2459069-02 .2655209-02 .2858234-02 .3068889-02 .3288960-02 .3518443-02 .3755323-02 .4005866-02 .4269697-02 .4547898-02
```

Continued on next page

Table 4 – continued from previous page

Sample Data Output

```
.4844697-02 .5157416-02 .5493968-02 .5856722-02 .6249363-02 .6676468-02 .7151910-02 .7680163-02 .8278725-02 .8971330-02
.9737482-02 .1083580-01 .1225605-01 .1392110-01 .1465606-01 .1476369-01 .1487130-01 .1497891-01 .1508652-01 .1519400-01
.1530174-01 .1540940-01 .1552457-01 .1659306-01 .1756156-01 .2046704-01 .2337252-01 .4080540-01 .6695473-01 .9310405-01
.1194060-00 .1323280-00 .1715520-00 .1911640-00 .2107760-00 .2303880-00 .2500000-00

STEADY STATE VALUES FOR MBAR AND G AT END OF BED
 MBAR= .12115+02 G= .30000+01

***** OPERATIONS COMPLETE *****
```

3.2 Two-Dimensional Steady-State Model

3.2.1 Input Description

The following is a description of the necessary input for the two-dimensional steady-state computer program. The input format is given in Table II. The coding of the sample data case for this program is shown in Figs. 4a and 4b, and a listing of the input data punch cards corresponding to this sample data case is shown in Figs. 5a and 5b. The statement numbers in the text below refer to the card numbers (first column) of Table II. For each run there will be only one card number one. Cards two through twenty-one should be included for each data case to be run.

1. The first card contains the number **NCASE**. This number indicates the number of data cases with each run. $1 \leq \text{NCASE} \leq 999$.

2. The second card is the **title card** used for individual data case identification. The title may be any alpha numeric information desired.

3. The third card contains the indicators **NRINGS** and **NOFZ**. **NRINGS** indicates the number of evenly spaced radial stations at which calculations are to be made where radial station number one is that one nearest the center of the reactor and radial station number (NRINGS) is that station nearest the reactor wall. For typical runs, **NRINGS** = 10 was found adequate to insure good results. Increasing this number would allow more detailed radial analysis, but it would also increase computer run time. **NOFZ** is the number of axial stations (Z's) to be used in the three tables input on cards 10 through 21.

4. Cards four contain the values of **F(I)**, (the rates of feed of hydrazine from buried injectors (Ref. 1) into the system in $lb/ft^3 - sec$). One value of F for each radial station (total number of radial stations = NRINGS) should be input. Ten numbers are allowed to a card. For the suggested NRINGS of 10, there would be one card with ten values of F.

5. Cards five contain the values of **GO(I)**, (the inlet mass flow rates in lb/ft^2-sec) for each radial station. Ten numbers are allowed to a card. For the suggested NRINGS of 10, there would be one card with ten values of GO. All values of GO must be greater than zero.

6. Cards six contain the values of **ZO(I)**, (the axial distance to the end of a buried injector in ft) for each radial station. Ten numbers are allowed to a card. For the suggested NRINGS of 10, there would be one card with ten values of ZO.

7. The seventh card contains the eight constants **ALPHA3**, **HF**, **R**, **MN2H4**, **MNH3**, **MN2**, **MH2**, and **ALPHAL**.

   - **ALPHA3** is the preexponential factor in the rate equation for the thermal decomposition of hydrazine. It equals $2.14 \times 10^{10} sec^{-1}$.
   - **HF** is the enthalpy of liquid hydrazine entering the bed in deg R.
   - **R** is the gas constant. It equals 10.73 (psia-ft^3)/(lb-mole-deg R).
   - **MN2H4** is the molecular weight of hydrazine. It equals 32.048 lb/lb mole.
   - **MNH3** is the molecular weight of ammonia. It equals 17.032 lb/lb mole.
   - **MN2** is the molecular weight of nitrogen. It equals 28.016 lb/lb mole.
   - **MH2** is the molecular weight of hydrogen. It equals 2.016 lb/lb mole.
   - **ALPHAL** is the preexponential factor in the rate equation for the catalytic decomposition of hydrazine. For the Shell 405 catalyst it equals $10^{10} sec^{-1}$.

8. The eighth card contains the eight constants **ALPHA2**, **AGM**, **BGM**, **KP**, **TF**, **CF**, **NMAX1**, and **NMAX2**.

   - **ALPHA2** is the preexponential factor in the rate equation for the catalytic decomposition of ammonia. For the Shell 405 catalyst it equals $10^{11} sec^{-1}$.

- **AGM** is the activation energy for the catalytic decomposition of hydrazine, divided by the gas constant. For the Shell 405 catalyst it equals 2,500 deg R.
- **BGM** is the activation energy for the catalytic decomposition of ammonia, divided by the gas constant. For the Shell 405 catalyst it equals 50,000 deg R.
- **KP** is the effective thermal conductivity of the porous catalyst particle. For the Shell 405 catalyst it equals 0.4×10^{-4} Btu/ft-sec-deg R.
- **TF** is the temperature of liquid hydrazine entering the bed in deg R.
- **CF** is the specific heat of liquid hydrazine. It equals 0.7332 Btu/lb-deg R.
- **NMAX1** is the constant used to determine the size of axial station increments in the liquid region. It equals 200. Increasing this number would result in a decrease in size of axial station increments (and an increase in computer run time).
- **NMAX2** is the constant used to determine the size of axial station increments in the liquid-vapor region. It equals 40. Increasing this number would result in a decrease in size of axial station increments (and an increase in computer run time).

9. The ninth card contains the inlet value of **P** and five constants **ZEND**, **DON2H4**, **DONH3**, **CGM**, and **RADIUS**.
   - **P** is the inlet chamber pressure in psia.
   - **ZEND** is the catalyst bed length in feet.
   - **DON2H4** is the diffusion coefficient of hydrazine in the gas phase at STP. It equals $0.95 \times 10^{-4} ft^2/sec.$
   - **DONH3** is the diffusion coefficient of ammonia in the gas phase at STP. It equals $0.17 \times 10^{-3} ft^2/sec.$
   - **CGM** is the activation energy for the thermal decomposition of hydrazine, divided by the gas constant. It equals 33,000 deg R.
   - **RADIUS** is the radius of the catalyst bed in feet.
10. Cards ten through thirteen contain **AVSZ(I)**, the bivariate interpolation table used to obtain the catalyst particle radius, $A(z, r)$.[4] These A values are obtained from subroutine UNBAR, an interpolation routine developed at the United Aircraft Research Laboratories, as functions of axial distance, Z, and radial distance, RAD. For this table there should be a total of (NOFZ) Z's, (NRINGS) RAD's and (NOFZ x NRINGS) A's. The table is set up as follows:
    - **CARD NO. 10**: This card contains the four table descriptors used by UNBAR. The first descriptor signifies the table number. For this program it equals 0.0. The second descriptor signifies the location in the array at which the table starts; the tables in this program are read in such that this number equals 1.0. The third descriptor for a bivariate table such as this one is the number of elements in the first set of independent variables in the table (in this case, the number of Z's). This number equals NOFZ. The fourth descriptor is the number of elements in the second set of independent variables in the table (in this case, the number of RAD's). This number equals NRINGS.
    - **CARD(S) NO. 11**: These cards contain the monatonically increasing Z values. Enough cards should be used to contain NOFZ values of Z at the rate of ten per card. For example, if $NOFZ = 12$, 12 values of Z should be input using 2 cards with ten values on the first card and the 2 remaining values on the second card.
    - **CARD(S) NO. 12**: These cards contain the monatonically increasing RAD's. Enough cards should be used to contain NRINGS values of RAD at the rate of ten per card.

[4] This variable is not subscripted in the program. This notation is used to show that the variable is a function of both axial distance and radial distance and to clarify the way the table is set up.

- **CARD(S) NO. 13**: These cards contain the values for $A(z,r)$. The A values are input at each Z value for all RAD's (i.e., (NRINGS) values of A for each Z) at the rate of ten per card. (See examples in text).

11. Cards 14 through 17 contain **APVSZ(I)**, the bivariate interpolation table used to obtain the catalyst particle surface area, $AP(z,r)$.[5] These AP values are obtained from UNBAR as functions of axial distance, Z, and radial distance, RAD, as in the AVSZ table discussed above. For this table there should be a total of (NOFZ) Z's, (NRINGS) RAD's, and (NOFZ x NRINGS) AP's. The table is set up as follows:

    - **CARD NO. 14**: This card is exactly the same as card 10.
    - **CARD(S) NO. 15**: These cards are exactly the same as cards 11.
    - **CARD(S) NO. 16**: These cards are exactly the same as cards 12.
    - **CARD(S) NO. 17**: These cards contain the values for $AP(z,r)$. These values are input at each Z value for all RAD's at the rate of ten values per card. (See examples in the discussion of the AVSZ table as the table setup is the same.)

12. Cards 18 through 21 contain **DELVSZ(I)**, the bivariate interpolation table used to obtain the inter-particle void fraction, DELTA (z,r).* These DELTA values are obtained from UNBAR as functions of axial distance, Z, and radial distance, RAD, as in the AVSZ table discussed above. For this table there should be a total of (NOFZ) Z's, (NRINGS) RAD's, and (NOFZ x NRINGS) DELTA's. The table is set up as follows:

    - **CARD NO. 18**: This card is exactly the same as card 10.
    - **CARD(S) NO. 19**: These cards are exactly the same as cards 11.
    - **CARD(S) NO. 20**: These cards are exactly the same as cards 12.
    - **CARD(S) NO. 21**: These cards contain the values for DELTA (z,r). These values are input at each Z value for all RAD's at the rate of ten values per card. (See examples in the discussion of the AVSZ table as the table setup is the same).

NOTE: The values for the orders of the decomposition reactions (called EN1, EN2, and EN3 in the one-dimensional model) are included in the equations in the two-dimensional model and therefore are not input.

[5] This variable is not subscripted in the program. This notation is used to show that the variable is a function of both axial distance and radial distance and to clarify the way the table is set up.

Table 5: Two-Dimensional Computer Program: Input Format (Table II)

CARD NUMBER	NUMBER OF CARDS	FORMAT FORTRAN	USED COLUMNS	SYMBOL OR DESCRIPTION	SYMBOL USED IN EQUATIONS	NOMENCLATURE
1	1	I3*	1-3	NCASE		Number of data cases
2	1	14A6	1-80	Title		
3	1	2I3*	1-3	NRINGS		Number of radial stations
			4-6	NOFZ		Number of Z's in input tables
4	**	10E8.4	1-8, 9-16, etc.	F(I)	F	Distributed Feed Rate
5	**	10E8.4	1-8, 9-16, etc.	GO(I)	G_0	Inlet mass flow rate
6	**	10E8.4	1-8, 9-16, etc.	ZO(I)	Z_0	Axial distance to injector end
7	1	8E10.5	1-10	ALPHA3	α_{hom}	Constant in rate equation
			11-20	HF	h_F	Enthalpy of feed
			21-30	R	R	Gas constant
			31-40	MN2H4	M^{N2H4}	Molecular weight of N2H4
			41-50	MNH3	M^{NH3}	Molecular weight of NH3
			51-60	MN2	M^{N2}	Molecular weight of N2
			61-70	MH2	M^{H2}	Molecular weight of H2
			71-80	ALPHAL	α_{het}^{N2H4}	Preexponential factor
8	1	8E10.5	1-10	ALPHA2	α_{het}^{NH3}	Preexponential factor
			11-20	AGM	Q_{het}^{N2H4}/R	Activation energy, deg R
			21-30	BGM	Q_{het}^{NH3}/R	Activation energy, deg R
			31-40	KP	K_p	Thermal conductivity
			41-50	TF	T_F	Feed temperature
			51-60	CF	C_F	Specific heat of liquid N2H4
			61-70	NMAX1		Determ. axial step size (liq. reg.)
			71-80	NMAX2		Determ. axial step size (liq. vap. reg.)
9	1	8E10.5	1-10	P	P	Inlet chamber pressure
			11-20	ZEND		Bed length
			21-30	DON2H4	D_0^{N2H4}	Diffusion coefficient of N2H4
			31-40	DONH3	D_0^{NH3}	Diffusion coefficient of NH3
			41-50	CGM	Q_{hom}^{N2H4}/R	Activation energy, deg R
			51-60	RADIUS		Bed radius
10	1	4E8.4	1-8	0.		Table descriptor
			9-16	1.		Table descriptor
			17-24	NOFZ.		Table descriptor
			25-32	NRINGS.		Table descriptor
11	*	10E8.4	1-8, 9-16, etc.	Z(I)	Z	Axial station
12	**	10E8.4	1-8, 9-16, etc.	RAD(I)	r	Radial station
13	***	10E8.4	1-8, 9-16, etc.	A(z,r)	a	Catalyst particle radius

Continued on next page

Table 5 – continued from previous page

CARD NUMBER	NUMBER OF CARDS	FORMAT FORTRAN	USED COLUMNS	SYMBOL OR DESCRIPTION	SYMBOL USED IN EQUATIONS	NOMENCLATURE
14	1	4E8.4	1-8	0.		Table descriptor
			9-16	1.		Table descriptor
			17-24	NOFZ.		Table descriptor
			25-32	NRINGS.		Table descriptor
15	*	10E8.4	1-8, 9-16, etc.	Z(I)	Z	Axial station
16	**	10E8.4	1-8, 9-16, etc.	RAD(I)	r	Radial station
17	***	10E8.4	1-8, 9-16, etc.	AP(z,r)	A_p	Total external catalyst particle surface area per unit volume of bed
18	1	4E8.4	1-8	0.		Table descriptor
			9-16	1.		Table descriptor
			17-24	NOFZ.		Table descriptor
			25-32	NRINGS.		Table descriptor
19	*	10E8.4	1-8, 9-16, etc.	Z(I)	Z	Axial station
20	**	10E8.4	1-8, 9-16, etc.	RAD(I)	r	Radial station
21	***	10E8.4	1-8, 9-16, etc.	DELTA(z,r)	δ	Interparticle void fraction

*All I format numbers should be right adjusted.
**Enough cards should be used to contain (NRINGS) values at the rate of ten per card.
***Enough cards should be used to contain (NRINGS) values for each Z at the rate of ten per card (see detailed example in text).

List of Symbols

Symbol	Description
a	Radius of spherical particle, ft
A_p	Total external surface of catalyst particle per unit volume of bed, ft^{-1}
c_i	Reactant concentration in interstitial fluid, lb/ft^3
c_p	Reactant concentration in gas phase within the porous particle, lb/ft^3
C_F	Specific heat of fluid in the interstitial phase, Btu/lb deg R
$\overline{C}_F$	Average specific heat of fluid in the interstitial phase, Btu/lb deg R
D_i	Diffusion coefficient of reactant gas in the interstitial fluid, ft^2/sec
D_0	Diffusion coefficient of reactant gas in the interstitial fluid at STP, ft^2/sec
D_p	Diffusion coefficient of reactant gas in the porous particle, ft^2/sec
f_i	Weighting factor in Eq. (I-11)
F	Rate of feed of hydrazine from buried injectors into the system (Ref. 1), $lb/ft^3 - sec$
g_c	Conversion factor, (lbm/lbe) ft/sec^2
G	Mass flow rate, $lb/ft^2 - sec$
h	Enthalpy, Btu/lb
h_c	Heat transfer coefficient, Btu/ft^2-sec-deg R
H	Heat of reaction (negative for exothermic reaction), Btu/lb
k_c	Mass transfer coefficient, ft/sec
k_0	Reaction rate constant, equals $\alpha e^{-\gamma}$
K_p	Thermal conductivity of the porous catalyst particle, Btu/ft-sec-deg R
M	Molecular weight, lb/lb mole
$\overline{M}$	Average molecular weight, lb/lb mole
n	Order of decomposition reaction
N_r	Radial mass flux, lb/ft^2-sec
P	Chamber pressure, psia
q_r	Radial heat flux, $Btu/ft^2 - sec$
Q_{het}	Activation energy for (heterogeneous) chemical reaction on the catalyst surfaces, Btu/lb mole
Q_{hom}	Activation energy for (homogeneous) chemical reaction in the interstitial phase, Btu/lb mole
r	Radial distance from the center of the cylindrical reaction chamber, ft
r_{het}	Rate of (heterogeneous) chemical reaction on the catalyst surfaces, $lb/ft^3 - sec$
r_{hom}	Rate of (homogeneous) chemical reaction in the interstitial phase, $lb/ft^3 - sec$
R	Gas constant, equals 10.73 psia ft^3/lb mole deg R, or, Radius of reactor
T	Temperature, deg R
T_{vap}	Vaporization temperature, deg R
w_i	Weight fraction of reactant in interstitial phase
x	Radial distance from the center of the spherical catalyst particle, ft
x_0	Defined in Appendix I (Discussion of Subroutine SGRAD)
z	Axial distance, ft
z_0	Axial distance to the end of buried injectors, ft
α	Preexponential factor in rate equation
β	Equals $[-(c_p)_s H D_p]/[K_p(T_p)_s]$
γ	Equals $Q_{het}/[R(T_p)_s]$
δ	Interparticle void fraction
ϵ	Eddy diffusivity, ft^2/sec
λ	Eddy conductivity, Btu/ft-sec-deg R
μ	Viscosity of interstitial fluid, lb/ft sec
ρ_i	Density of interstitial fluid, lb/ft^3

Continued on next page

Table 6 – continued from previous page

Symbol	Description
Subscripts	
F	Refers to feed
i	Refers to interstitial phase
P	Refers to gas within the porous catalyst particle
s	Refers to surface of catalyst particle
Superscripts	
j	Refers to chemical species
L	Refers to liquid at vaporization temperature
V	Refers to vapor at vaporization temperature

A Description of Subroutines

The following is a list and brief description of the subroutines which comprise the UNIVAC 1108 computer programs describing the one and two-dimensional steady-state models of a hydrazine catalytic reactor. Subroutine SGRAD, since it is the key subroutine in each program is described in detail. The flow charts for the main programs and major subroutines are included immediately after this list in Figs. I-l through I-8. The number outside of and next to any block on the flow charts indicates the approximate statement number in that routine at which that particular operation occurs.

One-Dimensional Model

MAIN (Fig. I-1) Controls input and calculates concentrations and temperatures in the liquid region of the reactor.

SLOPE (Fig. I-1) Calculates concentration and temperature profiles within the catalyst particles for the liquid and liquid vapor regions of the reactor. This subroutine is similar to SGRAD which is described in detail later in this section.

LQVP (Fig. 1-2) Calculates enthalpy during the liquid vapor region of the reactor (concentration of N2H4 and temperature remain constant).

LQV2 (Fig. 1-2) Calculates hydrazine concentration, enthalpy and temperatures during the liquid-liquid vapor region of the reactor (concentration of hydrazine varies).

VAPOR (Figs. 1-3 & 1-4) Calculates concentrations, temperatures and pressures in the vapor region of the reactor.

PARAM (Fig. 1-5) Calculates parameters needed for calculations done in subroutine SLOPE.

CONC (Fig. 1-5) Calculates reactant concentrations at the liquid vapor-vapor interface of the reactor.

UNBAR Interpolation routine used to obtain values from a table.

BLOCK DATA TABLES Tables of:

1. temperature vs. viscosity
2. temperature vs. vapor pressure
3. temperature vs. heats of reaction
4. temperature vs. specific heat
5. vapor pressure vs. temperature
6. enthalpy vs. temperature

SGRAD (Fig. 1-5) This routine is the same as it is in the two-dimensional model. For a detailed description, see the section describing two-dimensional subroutines.

Two-Dimensional Model

MAIN (Fig. 1-6) Controls input and calculates concentrations and temperatures in the liquid region of the reactor for all annular regions.

SLOPE (Fig. 1-6) Calculates concentration and temperature profiles within the catalyst particles for the liquid and liquid vapor regions of the reactor for all annular regions. This subroutine is similar to SGRAD which is described in detail later in this section.

LQVP (Fig. 1-6) Calculates enthalpy during the liquid vapor region of the reactor for all annular regions (concentration of N_2H_4 and temperature remain constant).

VAPOR (Fig. 1-7) Calculates concentrations, temperatures and pressures in the vapor region of the reactor for all annular regions.

DELTAZ (Fig. 1-8) Calculates axial increments for the vapor region.

ORDER (Fig. 1-8) Arranges an array of numbers in ascending order.

UNBAR Interpolation routine used to obtain values from a table.

BLOCK DATA TABLES Tables of:

1. temperature vs. viscosity
2. temperature vs. vapor pressure
3. temperature vs. heats of reaction
4. temperature vs. specific heat
5. vapor pressure vs. temperature
6. enthalpy vs. temperature

SGRAD (Fig. 1-8) Detailed description follows:

SGRAD (Fig. 1-8)

The purpose of subroutine SGRAD is to solve the implicit integral equations describing reactant concentration and temperature profiles in the porous catalyst particles and to calculate the slope of the reactant concentration gradient at the surface of the catalyst particles. This routine is used for calculations in the vapor region of the reactor only. In the hydrazine catalytic reactor system, ammonia concentration profiles are calculated but the subroutine is very general and can be used for many other reactants. The key equation to be solved is an implicit integral equation of the form (Refs. 2 and 9):

$$\begin{aligned} c_p^{NH_3}(x/a) = c_i^{NH_3} - a^2 \left[\frac{1}{x/a} - \frac{ak_c^{NH_3} - D_p^{NH_3}}{ak_c^{NH_3}} \right] \int_{x_0/a}^{x/a} \xi^2 \frac{r_{het}^{NH_3}[c_p^{NH_3}(x/a)]}{D_p^{NH_3}} d\xi \\ -a^2 \int_{x/a}^{1} \left[\frac{1}{\xi} - \frac{ak_c^{NH_3} - D_p^{NH_3}}{ak_c^{NH_3}} \right] \xi^2 \frac{r_{het}^{NH_3}[c_p^{NH_3}(x/a)]}{D_p^{NH_3}} d\xi \end{aligned} \tag{37}$$

where $c_p^{NH_3}(x)$ is the reactant (ammonia) concentration as a function of x (the radial position within the catalyst particle), $c_i^{NH_3}$ is the interstitial reactant concentration and a is the radius of the spherical catalyst particle. To solve this equation, a two-phase iterative scheme is used. First, an initial estimate for $c_p^{NH_3}(x)$ is found through an iterative method of calculating successively better approximations. Second, using the good initial estimate found in the first phase, a similar iterative method is used to arrive at converged values of the actual $c_p^{NH_3}(x)$ distribution.

Phase I

It was found through hand calculation that solutions of Eq. (37) were very likely to diverge if the initial estimate was not a very good estimate. Therefore, in the first phase of this subroutine the iterative scheme is used to find this good first estimate. A linear function of the type shown in Fig. I-9 was found to be a fairly close approximation to the actual concentration distribution. The point at which the reactant concentration profile changes slope is referred to as x_0.

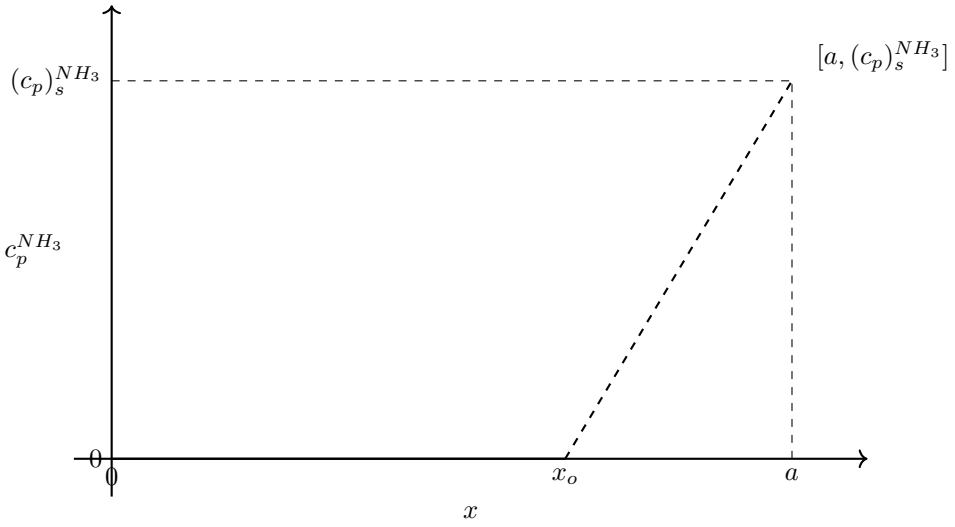

Figure 1: Figure I-9: Linear Approximation of Concentration Profile

The final solution to Phase I is a distribution of this type.

Iterative Procedure: Phase I

1. First a guess is made at a value for the reactant concentration at the surface of the catalyst particle: $(c_p)_s^{NH_3} = c_i^{NH_3}/2$.

2. Using this value, a value is found for the slope of the concentration profile at the surface, $[dc_p^{NH_3}/dx]_{x=a}$.

$$\left[\frac{dC_p^{NH_3}}{dx}\right]_{x=a} = \frac{k_c^{NH_3}}{D_p^{NH_3}}\left[c_i - (c_p)_s\right]^{NH_3} \tag{38}$$

   where $k_c^{NH_3}$ is calculated from an equation given in Ref. 1 and $D_p^{NH_3}$ is calculated from Eq. (39).

$$D_p^{NH_3} = D_0^{NH_3}\left\{\left(\frac{(T_p)_s}{492}\right)^{1.823}\cdot\left(\frac{14.7}{P}\right)\cdot\left[1 - e^{-0.0672(P/14.7)(492/(T_p)_s)}\right]\right\} \tag{39}$$

3. The temperature at the particle surface, $(T_p)_s$, is calculated from

$$(T_p)_s = T_i - \frac{1}{h_c}\left[(H\cdot k_c\cdot c_i)^{N_2H_4} + (H\cdot D_p\cdot[dc_p/dx]_{x=a})^{NH_3}\right] \tag{40}$$

   where T_i and $c_i^{N_2H_4}$ are input to the subroutine, $H^{N_2H_4}$ and H^{NH_3} are taken from tables in the computer program, and h_c and $k_c^{N_2H_4}$ are calculated according to the equations in Ref. 1.

4. Using the point $[a, (c_p)_s^{NH_3}]$ and the slope $[dc_p^{NH_3}/dx]_{x=a}$, a line is established and extrapolated to the $c_p^{NH_3} = 0$ axis, intersecting the line at x_0 (as in Fig. I-9).

5. The value for x_0 is calculated from

$$x_0 = a - \left\{ \frac{(c_p)_s}{[dc_p/dx]_{x=a}} \right\}^{NH_3} \tag{41}$$

Since the region of primary interest is the particle surface, it is at this point that convergence on a value for $c_p^{NH_3}(x)$ is tested. To test for convergence, a new $(c_p)_s^{NH_3}$ is calculated and compared to the previous $(c_p)_s^{NH_3}$. The new value for $(c_p)_s^{NH_3}$ can be calculated from Eq. (37) by noting that, at the catalyst particle surface, where $x = a$, the second integral term in Eq. (37) drops out leaving

$$(c_p)_s^{NH_3} = c_i^{NH_3} - \left[\frac{1}{X} - \frac{ak_c - D_p^{NH_3}}{a^2 k_c^{NH_3}} \right] \int_0^a \xi^2 \frac{r_{het}[c_p^{NH_3}(x)]}{D_p^{NH_3}} d\xi \tag{42}$$

As can be seen in Fig. (I-9) in distributions of this type all values of $c_p^{NH_3}(x)$ between 0 and x_0 are zero. Therefore, in evaluating the integrals, all points between 0 and x_0 can be ignored. If this is done and if x is normalized by dividing by a, Eq. (42) reduces to

$$(c_p)_s^{NH_3} = c_i^{NH_3} - a^2 \left[1 - \frac{ak_c^{NH_3} - D_p^{NH_3}}{ak_c^{NH_3}} \right] \int_{x_0/a}^1 \xi^2 \frac{r_{het}[c_p^{NH_3}(x)]}{D_p^{NH_3}} d\xi \tag{43}$$

where all terms have been previously determined except r_{het} which is calculated from

$$r_{het}^{NH_3} = k_0 (c_i^{NH_3})^{1-n} \cdot [c_p^{NH_3}(x)]^n \exp \left\{ \frac{\gamma\beta(1 - c_p^{NH_3}(x)/c_i^{NH_3})}{[1 + \beta(1 - c_p^{NH_3}(x)/c_i^{NH_3})]} \right\} \tag{44}$$

where n, k_0, γ, and β are defined in the List of Symbols.

6. A new value for $(c_p)_s^{NH_3}$ is calculated using Eq. (43) where the integral is evaluated numerically using the trapezoidal method.

7. A new value for $[dc_p^{NH_3}/dx]_{x=a}$ is calculated from Eq. (38) using the newly calculated $(c_p)_s^{NH_3}$.

8. New values are calculated for $(T_p)_s$, $D_p^{NH_3}$, γ, β, k_0.

9. The following convergence tests are made:

$$\left| \frac{[T_i - (T_p)_s]_{OLD} - [T_i - (T_p)_s]_{NEW}}{[T_i - (T_p)_s]_{NEW}} \right| \leq 0.05 \tag{45}$$

and

$$\left| \frac{[c_i - (c_p)_s]_{OLD}^{NH_3} - [c_i - (c_p)_s]_{NEW}^{NH_3}}{[c_i - (c_p)_s]_{NEW}^{NH_3}} \right| \leq 0.05 \tag{46}$$

If these tests are both satisfied, the value of x_0 calculated in Eq. (41) is saved and the program moves on to Phase II.

If both tests are not satisfied, an averaged value of $(c_p)_s^{NH_3}$ is calculated using as many as three averaging techniques to insure rapid convergence. Using this new value of $(c_p)_s^{NH_3}$, steps 2 through 9 are repeated up to a maximum of twenty-five times. If no convergence is reached after twenty-five iterations, a "weighted" estimate of x_0 is tried:

$$x_0 = f_i(x_0)_{\text{previously calculated}} + (1 - f_i)(x_0)_{\text{last calculated}} \tag{47}$$

Steps 1 through 9 are repeated up to twenty-five times. Succeeding values $f_i = 0.80, 0.85, 0.90,$ and 0.95 are tried until convergence is reached. If convergence still is not reached and therefore a satisfactory x_0 is not found, a program termination with an appropriate error message follows.

Phase II

Using as an initial approximation the straight line determined by the convergent x_0 and $[dc_p^{NH_3}/dx]_{x=a}$ found in Phase I, an iterative scheme similar to that in Phase I is now employed to find convergent values for the entire $c_p^{NH_3}(x)$ distribution within the catalyst particle. It was found through hand calculations that the convergent values of $c_p^{NH_3}(x)$ near the surface were not changed by more than 5 percent when the values of $c_p^{NH_3}(x)$ between 0 and x_0 were not considered in the iterative procedure. Therefore, the points in this range are ignored.

Iterative Procedure: Phase II The values of $c_p^{NH_3}(x)$, $(T_p)_s$, $k_o^{NH_3}$, β^{NH_3}, γ^{NH_3}, etc. found in the last iteration in Phase I are the initial input to the following iteration.

1. A new $c_p^{NH_3}(x)$ profile is calculated from Eq. (48).

$$\begin{aligned} c_p^{NH_3}(x/a) = c_i^{NH_3} &- a^2 \left[\frac{1}{x/a} - \frac{ak_c^{NH_3} - D_p^{NH_3}}{ak_c^{NH_3}}\right] \int_{x_0/a}^{x/a} \xi^2 \frac{r_{het}^{NH_3}[c_p^{NH_3}(x/a)]}{D_p^{NH_3}} d\xi \\ &- a^2 \int_{x/a}^{1} \left[\frac{1}{\xi} - \frac{ak_c^{NH_3} - D_p^{NH_3}}{ak_c^{NH_3}}\right] \xi^2 \frac{r_{het}^{NH_3}[c_p^{NH_3}(x/a)]}{D_p^{NH_3}} d\xi \end{aligned} \tag{48}$$

As before, the limits of the integral have been normalized by dividing by a. The integrals are evaluated numerically using the finite sum approximation described below.

To evaluate the integral terms in Eq. (48) the following procedure, using a finite sum approximation, is used:

(a) the interval $x_0/a \le x/a \le 1$ is divided into 24 equally spaced subdivisions, and an average value for $r_{het}[c_p^{NH_3}(x/a)]$ is calculated for each of these divisions.

(b) treating $r_{het}[c_p^{NH_3}(x/a)]$ as constant over each of these subdivisions, Eq. (48) can be approximated by

$$\begin{aligned} C_p^{NH_3}(x/a) = c_i^{NH_3} &- \frac{a}{D_p^{NH_3}} \left[\frac{1}{x/a} - \frac{ak_c^{NH_3} - D_p^{NH_3}}{ak_c^{NH_3}}\right] \left\{ r_{het}^1 \int_{x_0/a}^{x_0/a+\Delta x/a} \xi d\xi \right. \\ &\left. + r_{het}^2 \int_{x_0/a+\Delta x/a}^{x_0/a+2\Delta x/a} \xi d\xi + \cdots + r_{het}^{24} \int_{x_0/a+(k-1)\Delta x/a}^{x_0/a+k\Delta x/a} \xi d\xi \right\} \\ &- \frac{a^2}{D_p^{NH_3}} \left\{ r_{het}^1 \int_{x_0/a+k\Delta x/a}^{x_0/a+(k+1)\Delta x/a} \left[\frac{1}{\xi} - \frac{ak_c^{NH_3} - D_p^{NH_3}}{ak_c^{NH_3}}\right] \xi^2 d\xi \right. \\ &+ r_{het}^2 \int_{x_0/a+(k+1)\Delta x/a}^{x_0/a+(k+2)\Delta x/a} \left[\frac{1}{\xi} - \frac{ak_c^{NH_3} - D_p^{NH_3}}{ak_c^{NH_3}}\right] \xi^2 d\xi + \dots \\ &\left. + r_{het}^{24} \int_{x_0/a+23\Delta x/a}^{x_0/a+24\Delta x/a} \left[\frac{1}{\xi} - \frac{ak_c^{NH_3} - D_p^{NH_3}}{ak_c^{NH_3}}\right] \xi^2 d\xi \right\} \end{aligned} \tag{49}$$

where $k = 1, 2, ..., 24$

(c) the integrals in Eq. (49) can now be evaluated directly viz

$$\int_a^b \xi d\xi = \frac{\xi^2}{2}\bigg|_a^b = \frac{b^2}{2} - \frac{a^2}{2}$$

$$\int_a^b \text{constant} \cdot \xi^2 d\xi = \text{constant} \cdot \frac{\xi^3}{3}\bigg|_a^b = \text{constant} \cdot \left(\frac{b^3}{3} - \frac{a^3}{3}\right)$$

(d) rearranging and integrating term by term in Eq. (49) yields the finite sum approximation for $c_p^{NH_3}(x/a)$ at each subdivision of the interval from x_0/a to 1:

$$C_p^{NH_3}(x/a)_{k+1} = C_i^{NH_3} - \frac{a^2}{D_p^{NH_3}} \left\{ \left(\frac{1}{x_k/a} - \frac{av+1}{av} \right) \right.$$
$$\sum_{j=1}^{k} \frac{r_{het}^{j}}{3} \left[\left(\frac{x_j}{a}\right)^3 - \left(\frac{x_{j-1}}{a}\right)^3 \right] + \sum_{j=k}^{24} \frac{r_{het}^{j+1}}{2} \left[\left(\frac{x_{j+1}}{a}\right)^2 - \left(\frac{x_j}{a}\right)^2 \right] \tag{50}$$
$$\left. - \left(\frac{av+1}{av} \right) \sum_{j=k}^{24} \frac{r_{het}^{j+1}}{3} \left[\left(\frac{x_{j+1}}{a}\right)^3 - \left(\frac{x_j}{a}\right)^3 \right] \right\}$$

where $v = (ak_c - D_p)^{NH_3}/ak_c^{NH_3}$ and $k = 1, 2, ..., 24$.

(e) the values for $c_p^{NH_3}(x/a)|_{x=x_0}$ and $c_p^{NH_3}(x/a)|_{x=a}$ are special cases where one or the other of the integral terms in Eq. (48) vanishes. Evaluation follows from a simple reduction of Eq. (50).

2. A new value for $[dc_p^{NH_3}/dx]_{x=a}$ is calculated from Eq. (38) using the newly calculated $(c_p)_s^{NH_3}$.

3. A new value for $(T_p)_s$ is calculated from Eq. (40).

4. Convergence tests are made (as they were in Phase I) using Eqs. (45) and (46).

   (a) If the convergence tests are both satisfied, the quantities GRAD and TGRAD are calculated according to Eqs. (51) and (52), and the program returns to the point from which the subroutine was called.

$$GRAD = [dC_p^{NH_3}/dx]_{x=a} \cdot D_p^{NH_3} \tag{51}$$

$$TGRAD = h_c[T_i - (T_p)_s] \tag{52}$$

   (b) If the tests are not both satisfied, a new $c_p^{NH_3}(x)$ distribution is calculated using one of various averaging techniques. Corresponding $[dc_p^{NH_3}/dx]_{x=a}$, $(T_p)_s$, x_0, γ, β, etc. are also calculated. Then steps 1 through 4 are repeated up to a maximum of 50 times. If convergence criteria are not met after 50 iterations, approximations to acceptable values of GRAD and TGRAD are made using the results of the Phase I iterative procedure, an appropriate message is printed, and the program returns to the point from which the subroutine was called.

Distributions of the type shown in Fig. (I-10) are typical of those found in this iterative procedure.

(1) converged linear approximation from Phase I

(2) curve calculated from curve (1) using Eq. (I-11) (Phase II, step 1)

(3) averaged curve calculated from curves (1) and (2) (Phase II, step 4b)

Appendix II: Listing of Computer Programs

One-Dimensional Steady-State Model

```
C ********************************************************************
C * *
C * DESCRIPTION OF INPUT DATA PUNCH CARDS FOLLOWS...                  *
C * *
C ********************************************************************
C
C CARD 1      COL'S 1-3   CONTAIN NCASE   (I3)    (ONLY ONE CARD 1 PER RUN)
C
```

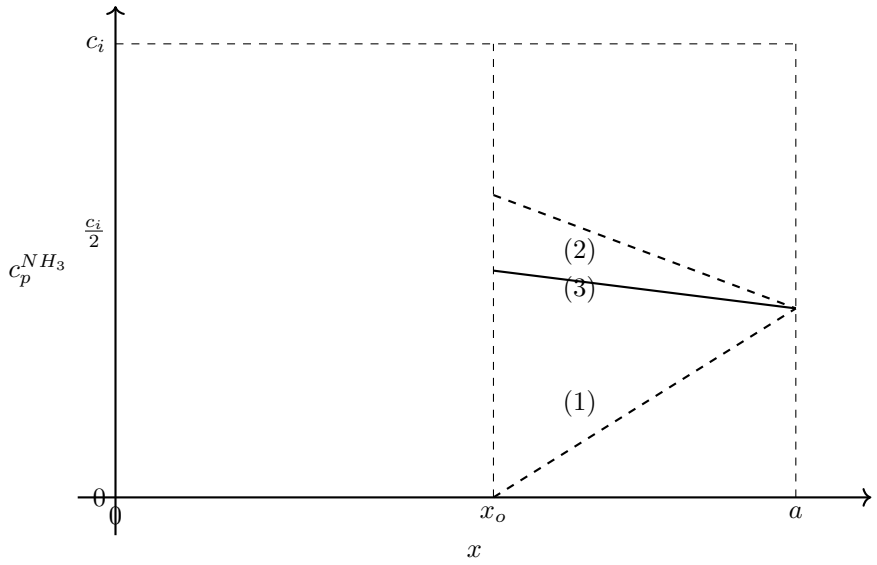

Figure 2: Figure I-10: Iterative Approximation of Concentration Profile

```
C (CARDS 2 THRU 16 SHOULD BE REPEATED FOR EACH DATA CASE)
C
C CARD 2       COL'S 1-80   TITLE CARD (14A6) ANY ALPHANUMERIC INFORMATION DESIRED
C
C CARD 3       COL'S 1-2    CONTAIN OPTION   (I2)
C              COL'S 3-4    CONTAIN PRINT    (I2)
C              COL'S 5-7    CONTAIN NOFZ     (I3)
C
C CARD 4       COL'S 1-10   CONTAIN ZO       (E10.5)
C              COL'S 11-20  CONTAIN GO       (E10.5)
C              COL'S 21-30  CONTAIN FC       (E10.5)
C              COL'S 31-40  CONTAIN ALPHA3   (E10.5)
C              COL'S 41-50  CONTAIN HF       (E10.5)
C              COL'S 51-60  CONTAIN R        (E10.5)
C              COL'S 61-70  CONTAIN WM4      (E10.5)
C              COL'S 71-80  CONTAIN WM3      (E10.5)
C
C CARD 5       COL'S 1-10   CONTAIN WM2      (E10.5)
C              COL'S 11-20  CONTAIN WM1      (E10.5)
C              COL'S 21-30  CONTAIN ALPHA1   (E10.5)
C              COL'S 31-40  CONTAIN ALPHA2   (E10.5)
C              COL'S 41-50  CONTAIN AGM      (E10.5)
C              COL'S 51-60  CONTAIN BGM      (E10.5)
C              COL'S 61-70  CONTAIN KP       (E10.5)
C              COL'S 71-80  CONTAIN CGM      (E10.5)
C
C CARD 6       COL'S 1-10   CONTAIN TF       (E10.5)
C              COL'S 11-20  CONTAIN CFL      (E10.5)
C              COL'S 21-30  CONTAIN ENMX1    (E10.5)
C              COL'S 31-40  CONTAIN ENMX2    (E10.5)
C              COL'S 41-50  CONTAIN ENMX3    (E10.5)
C              COL'S 51-60  CONTAIN DIF3     (E10.5)
C              COL'S 61-70  CONTAIN DIF4     (E10.5)
C              COL'S 71-80  CONTAIN PRES     (E10.5)
C
C CARD 7       COL'S 1-10   CONTAIN ZEND     (E10.5)
```

```
C              COL'S 11-20 CONTAIN EN1     (E10.5)
C              COL'S 21-30 CONTAIN EN2     (E10.5)
C              COL'S 31-40 CONTAIN EN3     (E10.5)
C
C (THE TABLE FOR CATALYST PARTICLE RADIUS VS
C  AXIAL DISTANCE ALONG REACTOR BED FOLLOWS)
C
C CARD 8       COL'S 1-8   CONTAIN THE NUMBER 0.0      (E8.4)
C              COL'S 9-16  CONTAIN THE NUMBER 1.0      (E8.4)
C              COL'S 17-24 CONTAIN NOFZ (FLOATING POINT) (E8.4)
C              COL'S 25-32 CONTAIN THE NUMBER 0.0      (E8.4)
C
C CARDS 9A,9B...  CONTAIN THE AXIAL STATION Z VALUES  (10E8.4)
C              Z(1),Z(2),....Z(NOFZ)
C              10 PER CARD, COL'S 1-80
C
C CARDS 10A,10B... CONTAIN THE CATALYST PARTICLE RADII (10E8.4)
C              A(1),A(2),....A(NOFZ)
C              10 PER CARD, COL'S 1-80
C
C (THE TABLE FOR CATALYST PARTICLE SURFACE AREA
C  VS AXIAL DISTANCE ALONG REACTOR BED FOLLOWS)
C
C CARD 11      THIS CARD IS IDENTICAL TO CARD 8
C
C CARDS 12A,12B... THESE CARDS (OR SINGLE CARD) ARE IDENTICAL TO CARDS 9A,9B...
C
C CARDS 13A,13B... CONTAIN THE CATALYST PARTICLE SURFACE AREAS (10E8.4)
C              AP(1),AP(2),...AP(NOFZ)
C              10 PER CARD, COL'S 1-80
C
C (THE TABLE FOR INTERPARTICLE VOID FRACTION VS
C  AXIAL DISTANCE ALONG REACTOR BED FOLLOWS)
C
C CARD 14      THIS CARD IS IDENTICAL TO CARD 8
C
C CARDS 15A,15B... THESE CARDS (OR SINGLE CARD) ARE IDENTICAL TO CARDS 9A,9B...
C
C CARDS 16A,16B... CONTAIN THE INTERPARTICLE VOID FRACTIONS (10E8.4)
C              DELA(1),DELA(2),....DELA(NOFZ)
C              10 PER CARD, COL'S 1-80
C
REAL KP,K                                                              0
INTEGER OPTION,PRINT                                                  10
COMMON /FTZ/TBLVP(70),TBLH4(42),TBLH3(42),SHTBL1(34),SHTBL2(34),      20
1        SHTBL3(34),SHTBL4(34),ZTBLD(46),ZTBLAP(46),ZTBLA(46)         30
COMMON /CO/HL,HV,FC,TF,CFL,CGM,ENMX1,AGM,DIF3,DIF4,KP,PRES,G0,        40
1        WM4,WM3,WM2,WM1,ALPHA3,R,TVAP,ZEND,BGM,HF,DZ,ALPHA1,ALPHA2   50
2        ,ENMX2,ENMX3,EN1,EN2,EN3,H,RAT,MI                            60
COMMON /VAR/DERIV(250),DHDZ(250),Z(250)                               70
COMMON /TOLL/ALIM,OPTION,C1,C2,C3,C4,CAV,G,TEMP,AP,WMAV,Z0,           80
COMMON /MUVST/VISVST(30)                                              90
COMMON /FLAGS/MFLAG,KFLAG,PRINT                                      100
COMMON /IFCE00/IFC,GATZ0                                             110
COMMON /LIZTBL/DHVST(18),DHLVST(18)                                  120
COMMON /DAVTBL/VPTBL(44)                                             130
DIMENSION  TITLE(14)                                                 140
READ (5,700) NCASE                                                   150
700 FORMAT (I3)                                                         160
```

```
KOUNT=1                                                                 170
705 READ (5,608) TITLE                                                      180
608 FORMAT (14A6)                                                           190
WRITE (6,609) TITLE                                                     200
609 FORMAT (1H1,14A6//)                                                     210
IFC=1                                                                   220
READ (5,809) OPTION,PRINT,NOFZ                                          230
809 FORMAT (2I2,I3)                                                         240
READ (5,800) Z0,G0,FC,ALPHA3,HF,R,WM4,WM3,WM2,WM1,ALPHA1,ALPHA2,        250
X      AGM,BGM,KP,CGM,TF,CFL,ENMX1,ENMX2,ENMX3,DIF3,DIF4,PRES,ZEND,      260
X      EN1,EN2,EN3,                                                     270
800 FORMAT (8E10.5)                                                         280
NZTBL = 2*NOFZ+4                                                        290
NOFZ4 = NOFZ+4                                                          300
NOFZ5 = NOFZ4+1                                                         310
CALL UNBAR (VPTBL(1),1,PRES,0.,TVAP,KK)                                 320
CALL UNBAR (DHVST(1),1,TVAP,0.,DELHV,KK)                                330
CALL UNBAR (DHLVST(1),1,TVAP,0.,DELHL,KK)                               340
HL=(TVAP-TF)*CFL                                                        350
HV=HL+DELHV-DELHL                                                       360
GATZ0=G0+FC*Z0                                                          370
IF(FC.GT.0.)GO TO 837                                                   380
IFC=0                                                                   390
637 WRITE (6,600)                                                           400
600 FORMAT (52X,16H INPUT CONSTANTS/7X,102H HF       HL         HV          410
X       TF       TVAP     CFL      PRESSURE     KP     FC                 420
X       G0)                                                                 430
WRITE (6,601) HF,HL,HV,TF,TVAP,CFL,PRES,KP,FC,G0                        440
601 FORMAT (3X,10E11.6//)                                                   450
WRITE (6,602)                                                           460
602 FORMAT (7X,103H  R     ALPHA3    CGM    DIF3     DIF4                    470
X        WM4      WM3
X   WM2      WM1    ZEND)                              480
WRITE (6,601) R,ALPHA3,CGM,DIF3,DIF4,WM4,WM3,WM1,WM1,ZEND               490
WRITE (6,603)                                                           500
603 FORMAT (6X,113H  AGM    BGM    ALPHA1     ALPHA2    N1                  510
X   N2     N3    ENMX1    ENMX2    ENMX3      )                          520
WRITE (6,601) AGM,BGM,ALPHA1,ALPHA2,EN1,EN2,EN3,ENMX1,ENMX2,ENMX3       530
WRITE (6,617) Z0                                                        540
617 FORMAT (// 8X,'Z0' / 3X,E11.6)                                          550
READ (5,20) (ZTBLA(I),I=1,4)                                            560
20 FORMAT (4E8.4)                                                           570
READ (5,21) (ZTBLA(I),I=5,NOFZ4)                                        580
21 FORMAT (10E8.4)                                                      590
READ (5,21) (ZTBLA(I),I=NOFZ5,NZTBL)                                    600
READ (5,20) (ZTBLAP(I),I=1,4)                                           610
READ (5,21) (ZTBLAP(I),I=5,NOFZ4)                                       620
READ (5,21) (ZTBLAP(I),I=NOFZ5,NZTBL)                                   630
READ (5,20) (ZTBLD(I),I=1,4)                                            640
READ (5,21) (ZTBLD(I),I=5,NOFZ4)                                        650
READ (5,21) (ZTBLD(I),I=NOFZ5,NZTBL)                                    660
WRITE (6,604)                                                           670
604 FORMAT (///55X,13H Z VS A TABLE)                                        680
WRITE (6,22) (ZTBLA(I),I=1,4)                                           690
22 FORMAT (40X,4E13.5)                                                      700
WRITE (6,23) (ZTBLA(I),I=5,NOFZ4)                                       710
23 FORMAT (1X,10E13.5)                                                      720
WRITE (6,25)                                                            730
25 FORMAT ( / )                                                             740
```

```
WRITE (6,23) (ZTBLA(I),I=NOFZ5,NZTBL)                                    750
WRITE (6,24)                                                             760
24 FORMAT ( // )                                                             770
WRITE (6,606)                                                            780
606 FORMAT (54X,14H Z VS AP TABLE)                                           790
WRITE (6,22) (ZTBLAP(I),I=1,4)                                           800
WRITE (6,23) (ZTBLAP(I),I=5,NOFZ4)                                       810
WRITE (6,25)                                                             820
WRITE (6,23) (ZTBLAP(I),I=NOFZ5,NZTBL)                                   830
WRITE (6,24)                                                             840
WRITE (6,607)                                                            850
607 FORMAT (54X,14H Z VS DELTA TABLE)                                        860
WRITE (6,22) (ZTBLD(I),I=1,4)                                            870
WRITE (6,23) (ZTBLD(I),I=5,NOFZ4)                                        880
WRITE (6,25)                                                             890
WRITE (6,23) (ZTBLD(I),I=NOFZ5,NZTBL)                                    900
WRITE (6,613)                                                            910
613 FORMAT (18X, ****************************** ENTERING LIQUID            920
X REGION     ******************************)                             930
MFLAG=0                                                                  940
DZ=0.0                                                                   950
Z(1)=0.0                                                                 960
H=HF                                                                     970
II=2                                                                     980
850 Z(II)=Z(II-1)+DZ                                                         990
TEMP=TF+(H-HF)/CFL                                                      1000
CALL UNBAR (TBLVP(I),1,TEMP,0.,VP,KK)                                   1010
CN2H4=(VP*WM4)/(R*TEMP)                                                 1020
CALL UNBAR (TBLH4(I),1,TEMP,0.,H4,KK)                                   1030
CALL UNBAR (ZTBLAP(I),1,Z(II),0.,AP,KK)                                 1040
CALL UNBAR (ZTBLA(I),1,Z(II),0.,A,KK)                                   1050
CALL PARAM(TEMP,Z(II),1,CN2H4,H4,0,G,GMMA,K,DPA,BETA)                   1060
CALL SLOPE (CN2H4,GMMA,K,BETA,EN1,DERIV(II),DPA,A,DIF4)                 1070
IF(H-HL)777,776,777                                                     1080
776 IF(MI.GT.20)DERIV(II)=DERIV(II-1)                                        1090
777 DHDZ(II)=-(H4*DPA*AP*DERIV(II)+FC*(H-HF))/G                              1100
DZ=-H4/(ENMX1*DHDZ(II))                                                 1110
WRITE(6,820)                                                            1120
820 FORMAT (/39X,48H  Z    TEMP    H DHDZ)                                   1130
WRITE(6,860) Z(II),TEMP,H,DHDZ(II)                                      1140
860 FORMAT (/30X,4E15.6)                                                     1150
IF(H-HL) 874,1020,874                                                   1160
874 H=H+DHDZ(II)*DZ                                                          1170
IF(H-HL) 875,1020,1000                                                  1180
875 II=II+1                                                                  1190
GO TO 850                                                               1200
C       BACKSTEP TO L-L-V-BOUNDARY
1000 DZ=(HL-H)/DHDZ(II)+DZ                                                   1210
H=HL                                                                    1220
II=II+1                                                                 1230
GO TO 850                                                               1240
1020 IF(OPTION.EQ.2) CALL LQV2(H,Z(II),DERIV(II),II,DHDZ(II),TEMP,CN2H4) 1250
IF(OPTION.EQ.2) GO                                                      1260
TO 1021
CALL LQVP(H,Z(II),DERIV(II),II,DHDZ(II),TEMP)                           1270
C       START VAPOR REGION
1021 DZ=-H4/(ENMX2*DHDZ(II))                                                      1280
CALL VAPOR(TEMP,Z(II),II,DHDZ(II),DERIV(II),H)                          1290
KOUNT=KOUNT+1                                                           1300
```

```
IF(KOUNT.LE.NCASE) GO TO 705                                          1310
WRITE(6,102)                                                          1320
102 FORMAT (////41X,36H ***** OPERATIONS COMPLETE *****)                  1330
STOP                                                                  1340
END                                                                   1350
```

Listing 1: MAIN Program Listing

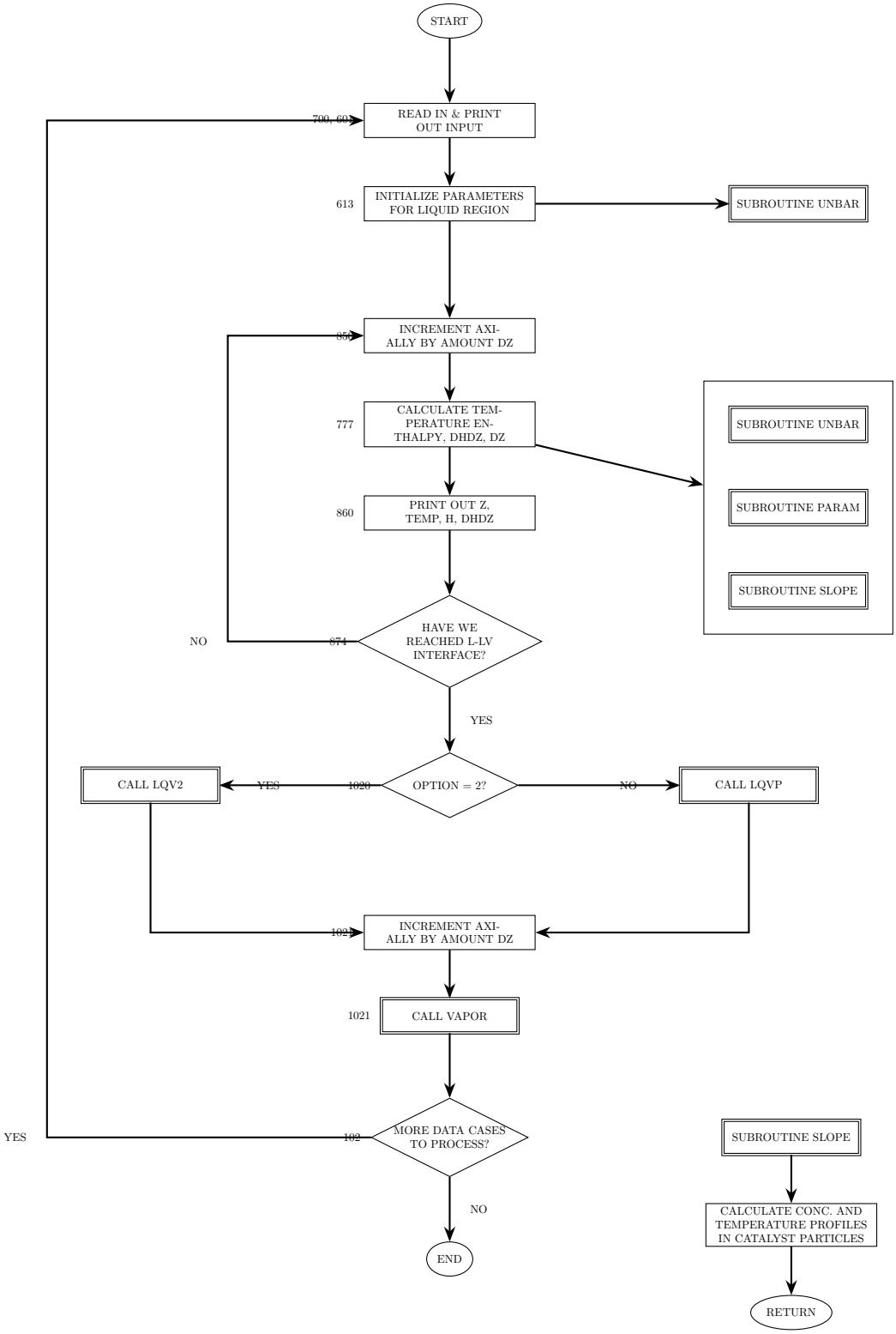

Figure 3: Figure I-1: MAIN PROGRAM and SUBROUTINE SLOPE Flow Diagrams

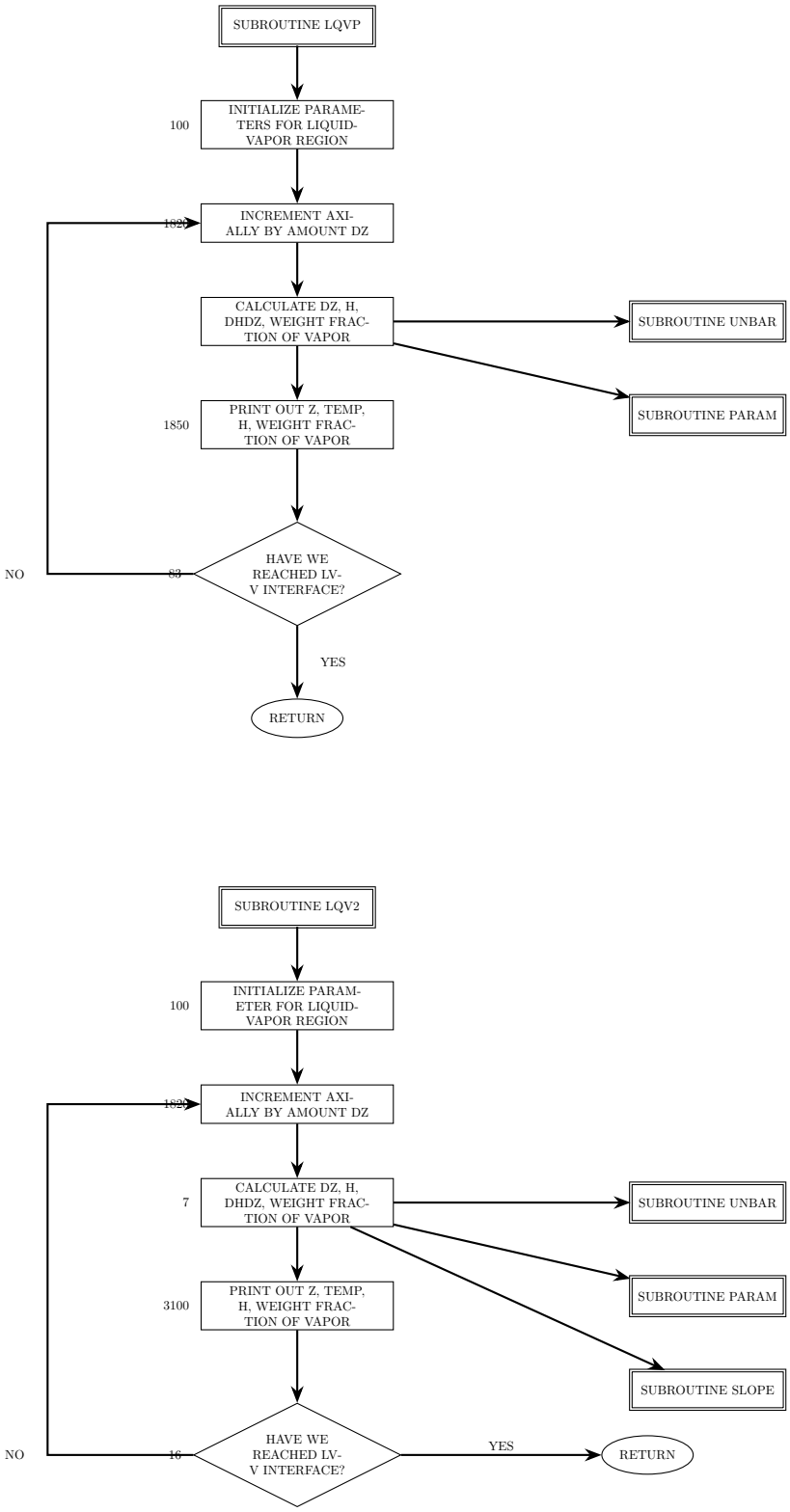

Figure 4: Figure I-2: SUBROUTINES LQVP and LQV2 Flow Diagrams

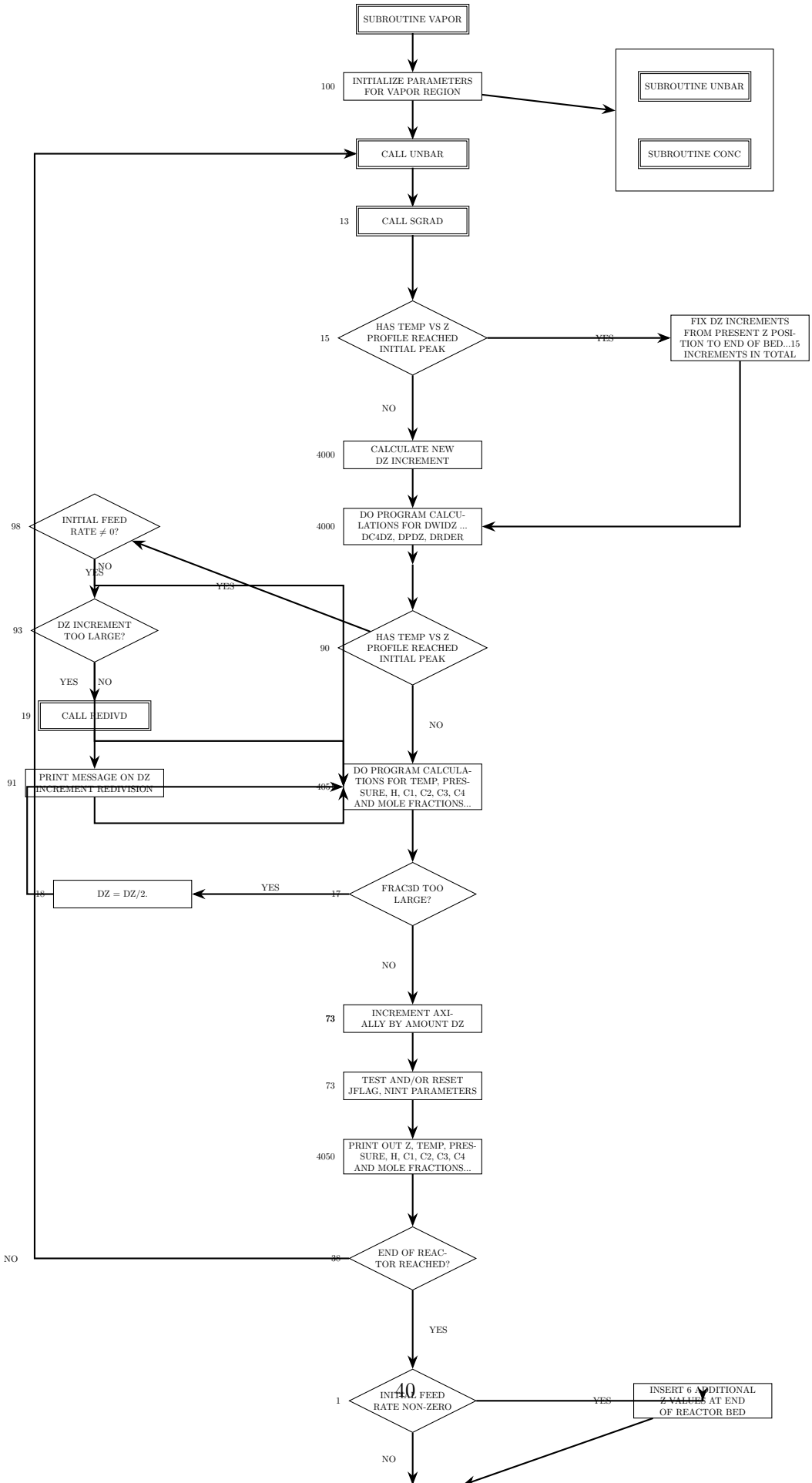
SUBROUTINE VAPOR
100
INITIALIZE PARAMETERS FOR VAPOR REGION
SUBROUTINE UNBAR
SUBROUTINE CONC
CALL UNBAR
13
CALL SGRAD
15
HAS TEMP VS Z PROFILE REACHED INITIAL PEAK
YES
FIX DZ INCREMENTS FROM PRESENT Z POSITION TO END OF BED...15 INCREMENTS IN TOTAL
NO
4000
CALCULATE NEW DZ INCREMENT
4000
DO PROGRAM CALCULATIONS FOR DWIDZ ... DC4DZ, DPDZ, DRDER
98
INITIAL FEED RATE ≠ 0?
NO
YES
YES
93
DZ INCREMENT TOO LARGE?
90
HAS TEMP VS Z PROFILE REACHED INITIAL PEAK
YES
NO
19
CALL REDIVD
NO
91
PRINT MESSAGE ON DZ INCREMENT REDIVISION
405
DO PROGRAM CALCULATIONS FOR TEMP, PRESSURE, H, C1, C2, C3, C4 AND MOLE FRACTIONS...
18
DZ = DZ/2.
YES
17
FRAC3D TOO LARGE?
NO
73
INCREMENT AXIALLY BY AMOUNT DZ
73
TEST AND/OR RESET JFLAG, NINT PARAMETERS
4050
PRINT OUT Z, TEMP, PRESSURE, H, C1, C2, C3, C4 AND MOLE FRACTIONS...
NO
38
END OF REACTOR REACHED?
YES
1
INITIAL FEED RATE NON-ZERO
YES
INSERT 6 ADDITIONAL Z VALUES AT END OF REACTOR BED
NO

B NASA9 Data File Format

This information is copied directly from the NASA-TP-2002-211556.pdf file. When I get to the bibliography work, I need to make sure it is added to the document.

Format for Thermodynamic Data Coefficients

This appendix explains the format for data contained in the file thermo.inp (app. D). Equations (1) to (3) are repeated here for convenience:

$$C_p^o(T)/R = a_1T^{-2} + a_2T^{-1} + a_3 + a_4T + a_5T^2 + a_6T^3 + a_7T^4 \quad (1)$$

$$H^o(T)/RT = -a_1T^{-2} + a_2 \ln T/T + a_3 + a_4T/2 + a_5T^2/3 + a_6T^3/4 + a_7T^4/5 + b_1/T \quad (2)$$

$$S^o(T)/R = -a_1T^{-2}/2 - a_2T^{-1} + a_3 \ln T + a_4T + a_5T^2/2 + a_6T^3/3 + a_7T^4/4 + b_2 \quad (3)$$

Table 7: TABLE C1.-FORTRAN FORMAT USED FOR DATA IN APPENDIX D

Record	Contents	FORTRAN format	Columns
		A16	1 to 16
1	Species name or formula	A62	19 to 80
	Comments and data sources		
2	Number of T intervals	I2	1 to 2
	Reference date code	A6	4 to 9
	Chemical formula-symbols (all capitals) and numbers	5(A2, F6.2)	11 to 50
	Zero for gas; nonzero for condensed	I2	51 to 52
	Molecular weight	F13.7	53 to 65
	Heat of formation at 298.15 K. J/mol	F15.5	66 to 80
3	Temperature range	2F11.3	1 to 22
	Number of coefficients for $C_p^o(T)/R$ (always seven)	I1	23
	T exponents in empirical equation for $C_p^o(T)/R$ [always -2,-1, 0, 1, 2, 3, 4; see eq. (1)]	8F5.1	24 to 63
	$H^o(298.15) - H^o(0)$ J/mol, if available	F15.3	66 to 80
4	First five coefficients for $C_p^o(T)/R$, eq. (1)	5D16.9	1 to 80
5	Last two coefficients for $C_p^o(T)/R$, eq. (1)	2D16.9	1 to 32
	Integration constants b_1 and b_2, eqs. (2) and (3)	2D16.9	49 to 80
Repeat 3, 4, and 5 for each interval			

Condensed phases are numbered in increasing order by temperature.
For example, the following data are for condensed titanium nitride:

```
1234567890123456789012345678901234567890123456789012345678901234567890123456789012345678901234567890
10        20        30        40        50        60        70        80
TiN(cr)         Chase, 1998 pp1612-4.                                        1
2 j 6/68 TI 1.00N 1.00      0.00      0.00      0.00 1  61.87374 -337648.800   2
200.000 800.0007 -2.0-1.0 0.0 1.0 2.0 3.0 4.0 0.0         5487.000            3
-5.479117220D+05 9.328691110D+03-6.386263890D+01 2.429925456D-01-4.304234520D-04    4
3.792645100D-07-1.317412256D-10                   -8.424256140D+04 3.392988560D+02   5
800.000 3220.0007 -2.0-1.0 0.0 1.0 2.0 3.0 4.0 0.0         5487.000            6
-3.656247060D+05 1.265730431D+03 3.831711190D+00 1.632900455D-03-1.062786626D-07    7
1.310931390D-11-5.770548410D-16                   -5.027654400D+04-1.652632899D+01   8
```

```
TiN(L)          Chase, 1998 pp1612-4.                                        9
1 j 6/68 TI 1.00N 1.00      0.00      0.00      0.00 2  61.87374 -337648.800  10
3220.000 6000.0007 -2.0-1.0 0.0 1.0 2.0 3.0 4.0 0.0         5487.000           11
0.000000000D+00 0.000000000D+00 7.548249987D+00 0.000000000D+00 0.000000000D+00   12
0.000000000D+00 0.000000000D+00                  -3.626039860D+04-3.958296649D+01  13
12345678901234567890123456789012345678901234567890123456789012345678901234567890
10        20        30        40        50        60        70        80
```